

JOURNAL OF THE AMERICAN CHEMICAL SOCIETY

Registered in U.S. Patent Office. © Copyright, 1976, by the American Chemical Society

VOLUME 98, NUMBER 21

OCTOBER 13, 1976

Excited Potential Energy Hypersurfaces for H_4 at Trapezoidal Geometries. Relation to Photochemical $2s + 2s$ Processes

Wolfgang Gerhartz,^{1a,b} Ronald D. Poshusta,^{1c} and Josef Michl^{*1b,d}

Contribution from the Department of Chemistry, University of Utah, Salt Lake City, Utah 84112, and the Chemical Physics Program, Washington State University, Pullman, Washington 99163. Received February 19, 1976

Abstract: Ab initio VB calculations, complete within minimum basis set (STO-4G), were performed on the Born–Oppenheimer potential surfaces of the three lowest singlet electronic states of the H_4 molecule for the three-dimensional subspace of all trapezoids. Perspective drawings of equipotential surfaces aid the visualization of the results. The hypersurface of the ground state is in excellent agreement with previous results and suggests that the transition state of the isotopic exchange reaction $H_2 + D_2 \rightleftharpoons 2HD$ lies outside the trapezoidal subspace. An exothermic reaction of singlet excited H_2 ($B^1\Sigma_u^+$) with ground state H_2 ($X^1\Sigma_g^+$) without activation energy and adiabatic formation of an H_4^* excimer is predicted. The bonding in the excimer is due to exciton resonance and charge transfer. The state is purely “zwitterionic”. However, at all energetically favorable excimer geometries, a purely dissociative state originating in overall singlet coupling of two parallel triplet H_2 molecules is almost degenerate with the excimer state, and this may limit the lifetime of the excimer. The dissociative doubly excited state is approximately half zwitterionic and half covalent and can also be viewed as originating in two crossed ground state H_2 molecules. Paths of steepest descent on this surface lead to $4H$, $H_2 + 2H$, or $2H_2$ (diagonal bonding). The case of $H_2 + H_2$ can be viewed as the simplest possible model for organic $2s + 2s$ processes. Our results support the picture outlined by van der Lugt and Oosterhoff for photochemical pericyclic processes (return to S_0 through a “pericyclic” minimum in a doubly excited state) and suggest answers to questions concerning photocycloadditions and other pericyclic processes: (i) the relation of the pericyclic minimum to the excimer minimum; (ii) the origin of activation energy; (iii) the physical factors affecting the ordering of excited states at the geometry of the pericyclic minimum; (iv) occurrence of diagonal bonding; (v) occurrence of excited product formation; (vi) relation of the photochemical process to triplet–triplet annihilation; (vii) its relation to radical ion recombination; and (viii) interrelation of the “supermolecule” correlation diagrams to interaction and correlation diagrams based on MO’s and states of partners in the photocycloaddition.

Born–Oppenheimer hypersurfaces for electronically excited singlet states in the six-dimensional nuclear configuration space of H_4 are of interest for several reasons. First, their availability might form a basis for eventual better understanding of processes such as collisional energy transfer, one of the simplest conceivable bimolecular photochemical reactions ($H_2 + H_2^* \rightarrow$ products), and one of the simplest molecular ion recombination reactions ($H_3^+ + H^- \rightarrow$ products). Although the last named reaction is one between two ground state species, it starts on an electronically excited surfaces of the total H_4 system and therefore has potential for production of H_2^* , particularly since excess energy can be carried away by H_2 so that no stabilization by a third body is needed. This type of process would be of interest as a new chemiluminescent and possibly chemical laser reaction.

Of the two processes, $H_2^* + H_2 \rightarrow$ products, and $H_3^+ + H^- \rightarrow$ products, the latter appears not to have been studied experimentally. Energy transfer between HD^* and H_2 has been investigated recently.² Previous theoretical work on the $H_2 + D_2$ exchange reaction has concentrated almost exclusively on

the ground state hypersurface and in spite of considerable effort expended^{3,4} there still appears to be an unreconciled gap between experimental and calculated activation energies (see ref 4 for a detailed recent discussion). Although the ground state process is not of prime concern to us, it is conceivable that insight into the nature of bonding in various electronic states of H_4 , which hopefully will emerge from our work, will suggest new possible pathways for the ground state exchange process as well. The most extensive study of H_4 potential surfaces including excited states prior to this was made by Rubinstein and Shavitt.^{3a} Their results are restricted to a very limited number of geometries (linear equidistant, square, 4:5 rectangles, 70° rhombus, and tetrahedral).

Second, the six-dimensional space of H_4 poses interesting methodological questions concerning investigations of surfaces in multidimensional spaces, such as problems of their touching (crossing) or near touching (avoided crossing), of their semi-empirical parameterization, and of suitable pictorial representations.

Finally, besides being interesting in its own right, H_4 also

Table I. Energy of H₂ in Its Ground State, X¹Σ_g⁺, and Excited State, B¹Σ_u⁺, as Computed by Various ab Initio Methods, and Exact Values

State	Method	R _{min} , Å	-E _{min} , au
X	MB	0.76	1.1479
	MBP	0.76	1.1489
	EBP	0.746	1.1548
	Exact (ref 11)	0.740	1.17447
B	MB	1.84	0.6736
	MBP	1.92	0.6795
	EBP	1.16	0.7307
	exact (ref 11)	1.28	0.7566

permits modeling of a great variety of systems with analogous topology important in organic photochemistry which, when simplified to the extreme, have as a common feature the involvement of four electrons on four atomic centers. Perhaps the largest class of such organic reactions is photochemical 2s + 2s pericyclic reactions,⁵ such as the butadiene to cyclobutene disrotatory ring closure or olefin cycloaddition. An improved knowledge of these in turn could help our understanding of "ground-state forbidden" photochemical processes in general. Thus, it is possible that a study of bonding forces in H₄ will eventually also contribute deeper qualitative insight into organic pericyclic processes, nature and reactivity of excimers, nature of singlet-singlet and doublet-doublet ion recombination reactions (modeled by H₃⁺ + H⁻ and H₂⁺ + H₂⁻, respectively), and nature of triplet-triplet annihilations (modeled by ³H₂ + ³H₂).

In this initial study, we explore the lowest three singlet states of H₄ at trapezoidal geometries, i.e., map a three-dimensional subspace, using a relatively simple method of calculation: full configuration interaction on a minimum basis set of Slater orbitals simulated as combinations of Gaussians with optimized exponents.

Method of Calculation

The choice of the computational procedure was governed by the following considerations. First, calculations must be cheap enough to permit a reasonably thorough mapping of the interesting regions of the whole six-dimensional space of H₄. Second, they must be reliable enough to produce qualitatively all features of the lowest excited states of the H₄ system likely to be important to us, such as nature of bonding in these states, existence of major reaction paths, approximate slopes of the hypersurfaces, areas of their touching and avoided touching, and areas of local minima. Third, they should preferably be simple enough to permit facile intuitive interpretation of the bonding and antibonding effects in simple terms which can be generalized to other systems.

We have selected a minimum basis set calculation with orbital exponents optimized separately for each state and each geometry, using the valence-bond (VB) formulation⁶ with inclusion of all terms (20 singlet terms, equivalent to full CI). The 1s Slater orbitals used were approximated as contractions⁷ of four Gaussian orbitals chosen to simulate a 1s hydrogenic orbital. This level of calculation will be referred to as MB. At geometries of D_{2h} and D_{4h} symmetries, exponents on all four atomic orbitals were assumed to be equal. In several instances a check was made by permitting them to differ. At all geometries in G and S states and at all geometries in the D state except those involving very small internuclear distances, all four exponents converged to the same value upon optimization (for state labels, see below).

At geometries of particular interest the wave functions were improved by "polarizing" the orbitals by floating the center of each member of a contraction (MBP).⁸ Calculations with

a fully optimized floating 1s 2s basis set were also performed at selected points in an attempt to determine the equilibrium geometry and vibrational frequencies of hydrogen excimer (H₄) and the results will be reported elsewhere⁹ (EBP, 29 symmetry adapted terms at C_{2v} geometries). The program has been used previously for molecules of type H_n⁺ and the reader is referred to ref 10 for details.

The choice of a minimum basis set imposes serious limitations on the reliability of the results and these will now be briefly discussed. First, atomic polarization is missing in the wave functions. This can, however, be supplied by floating the orbitals, as was done at selected geometries. No significant effects were discovered in this way. Second, intraatomic correlation is missing as well. Thus, H⁻ is calculated not to be bound, and all states in whose VB description ionic structures play a large role are probably described relatively poorly with respect to covalent states. Thus, a floating minimum basis set calculation for the B¹Σ_u⁺ state of H₂, well represented by H⁺H⁻ ↔ H⁻H⁺, yields a minimum near 1.84 Å at -0.6736 au, in error by 44% in bond length and 11% in energy from the exact calculation of Kolos and Wolniewicz¹¹ which gives 1.28 Å and -0.7566 au. This is to be compared with results for the largely covalent X¹Σ_g⁺ state of H₂, where the minimum basis set gives 0.76 Å and -1.1464 au, in error by 3% in bond length and 2% in energy from the exact results,¹¹ 0.74 Å and -1.17447 au. Our results for H₄ show similar trends for differences between minimum and extended basis set calculations. Also the comparison of results of ref 3a and 3c is instructive in this regard (a summary of our results for the ground and B states of H₂ by various methods is given in Table I). It thus appears almost certain that the energies of "ionic" states will be too high relative to those of "covalent" states and that possible minima in "ionic" states will appear at too large interatomic distances, and this will have to be kept in mind throughout.

The third main inadequacy of the minimum basis set approach is the inability to describe more than the lowest few states of H₄ and to provide proper dissociation limits for most states. Neither H nor H⁻ have any excited states in this approximation. In H₂, X¹Σ_g⁺ and b³Σ_u⁺ states are represented adequately, but B¹Σ_u⁺ and E¹Σ_g⁺ states are represented as hybrids of H⁺H⁻ and H⁻H⁺ at all distances, whereas in reality they dissociate to H + H*. Higher states such as C¹Π_u and a³Σ_g⁺ are missing altogether. Thus, the present results suggest various possible paths and should be viewed as a first step toward a theoretical investigation of the photochemical reaction H₂ + H₂* in the lower excited states but are not by themselves adequate for a definitive discussion.

In defense of the use of the minimum basis set, we also note that a general discussion of organic 2s + 2s processes needs to focus on states analogous to the lowest three states of H₄, which originate in the ground (X¹Σ_g⁺), the triplet (b³Σ_u⁺), and singlet (B¹Σ_u⁺) singly excited states of H₂. These processes are thus likely to be qualitatively correctly described at short and medium internuclear separations, particularly since we optimize exponents separately for each geometry and each state. In our VB wave functions, the degree of "ionic" character of each state at each geometry is clearly apparent, and we feel that this provides us with an adequate warning mechanism for estimating when small energy differences between two different surfaces are likely to be meaningful and when they are not. In the latter case, we proceed to 1s 2s basis set or, funds permitting, to 1s 2s 2p basis set calculations.

Results

All results here are for the MB level of calculation unless otherwise stated.

Graphical Presentation. For this work we confine our at-

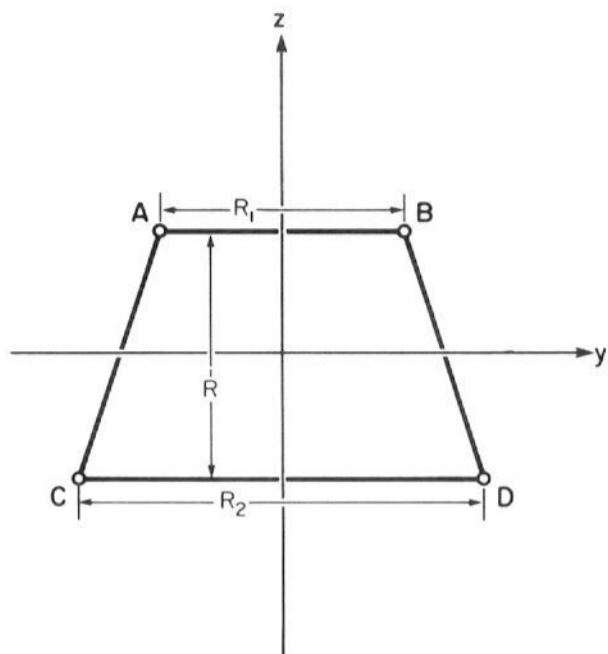


Figure 1. Coordinate system and molecular parameters of trapezoidal H_4 .

tention to trapezoidal geometries of H_4 in the three lowest singlet states. Three dimensions specify the geometry of such trapezoids: the lengths of the two parallel sides, R_1 and R_2 , and their separation R . These dimensions are defined by Figure 1. We have also labeled the nuclei A, B, D, and C at the vertices for convenience in the following discussion. It is convenient to use the conventional notation \overline{AB} , etc., to represent the distance between vertices (nuclei) A and B, etc. Thus, $R_1 = \overline{AB}$ and $R_2 = \overline{CD}$ in Figure 1.

The potential energy hypersurfaces of interest are denoted by $E_G(R_1, R_2, R)$, $E_S(R_1, R_2, R)$, and $E_D(R_1, R_2, R)$. Here the subscripts G, S, D refer to the ground state, singly excited state, and doubly excited state, respectively, as explained below. Four dimensions are required to plot $E(R_1, R_2, R)$. To permit visualization of these hypersurfaces, we show perspective views of equipotential surfaces (i.e., surfaces of constant E). A nested series of such isoenergetic surfaces, labeled with the appropriate energy values, is displayed for each of the three states in Figures 2 through 6. Such views are directly analogous to the common expedient of representing functions in two dimensions, $E(R_1, R_2)$, as contour maps. Atomic energy units are used (ionization energy of H atom is 0.5 au).

It is not possible to read energy values from Figures 2–6 with great accuracy. But then, there would be little point in a very accurate display of rather approximate results, except as a benchmark for future comparison with more accurate results, which will probably be done at selected points only. The surfaces are only approximate because of the limited nature of the basis set discussed above and because the grid used for their construction was relatively sparse, particularly in regions which appeared to be smooth or of little interest, in line with the general philosophy adopted (about 150 points for each state). The main purpose is a display of low-energy reaction paths, minima, barriers, and avoided crossings, and we believe that all such features shown in Figures 2–6 are semiquantitatively reliable. Details of slopes and absolute energy differences between surfaces of differing degree of ionicity are not reliable, particularly those of the excited singlets.

Results for the ground state G (A_1 symmetry in the C_{2v} group of a trapezoid) are displayed in Figures 2 and 3, which show two different views of the same set of equipotential surfaces. There are two low-lying excited singlet states, which we shall refer to as D and S (symmetries A_1 and B_2 , respectively, in the C_{2v} group of a trapezoid). Results for the D state are shown in Figure 4. Finally Figures 5 and 6 show two views of the surfaces for the S state. At large values of R , R_1 , and R_2 , there is more fine structure in the S hypersurfaces than is shown in Figures 5 and 6 as a result of touching and avoided

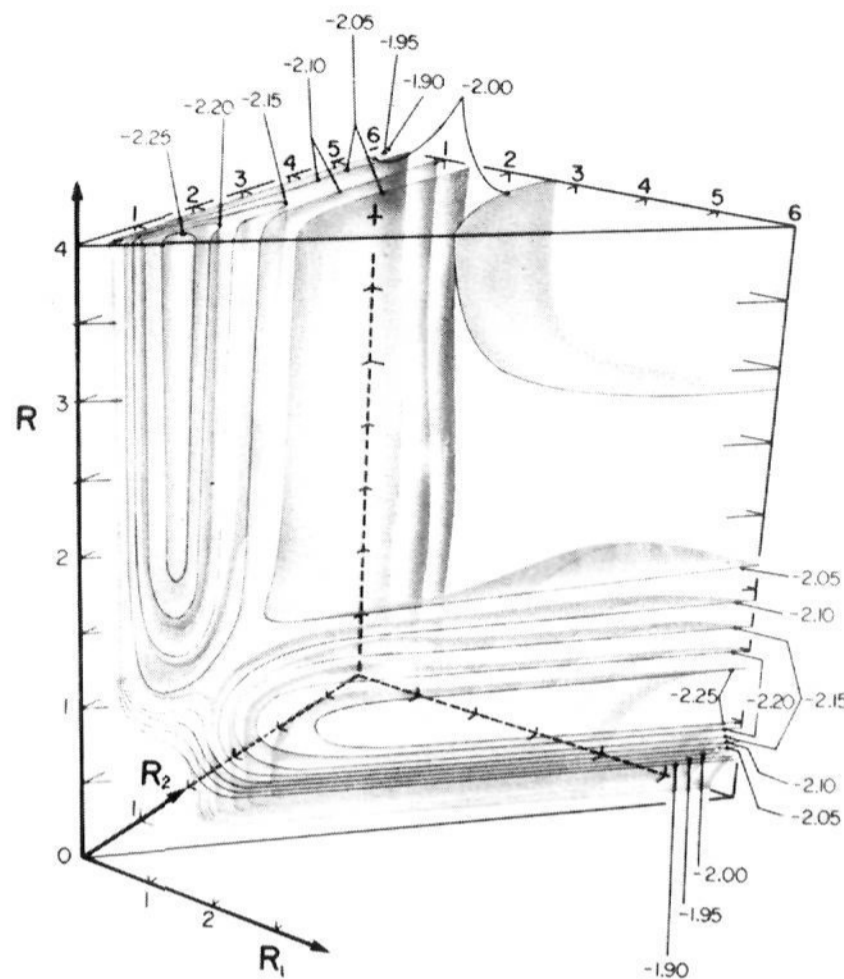


Figure 2. Equipotential surfaces of trapezoidal H_4 in the ground (G) state, viewed from the "front".

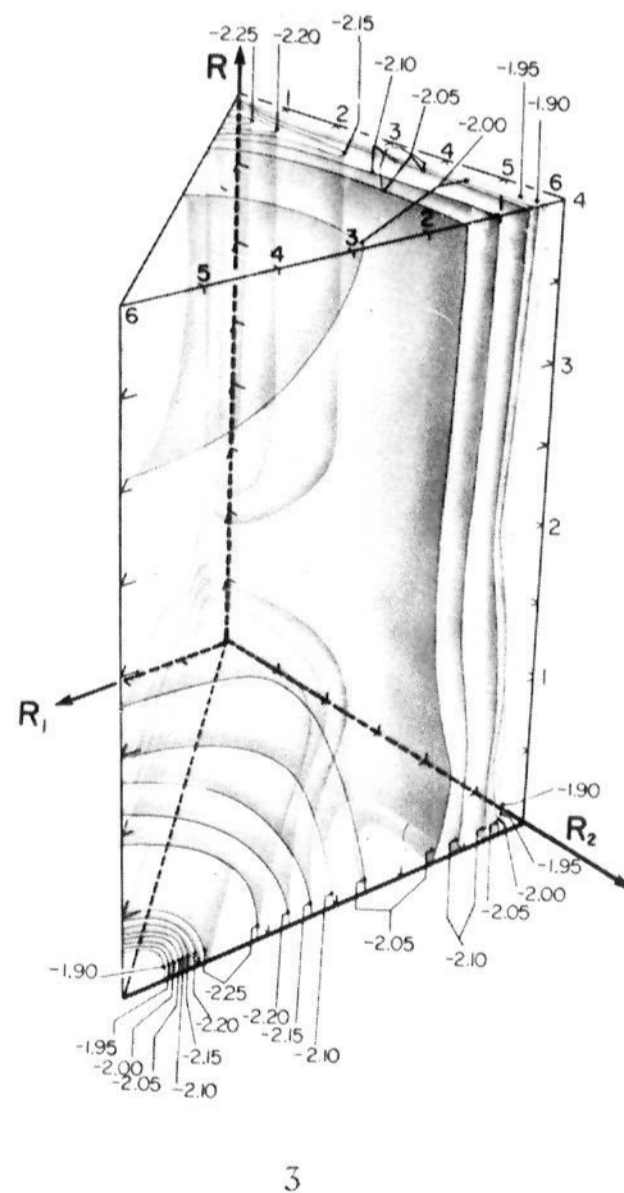


Figure 3. Equipotential surfaces of trapezoidal H_4 in the ground (G) state, viewed from the "rear".

touching with the next higher surface. This is readily seen in the limit of $R \rightarrow \infty$ for which results can be obtained from simple consideration of the potential energy curves of X and B states of H_2 . We are not displaying the details in this region

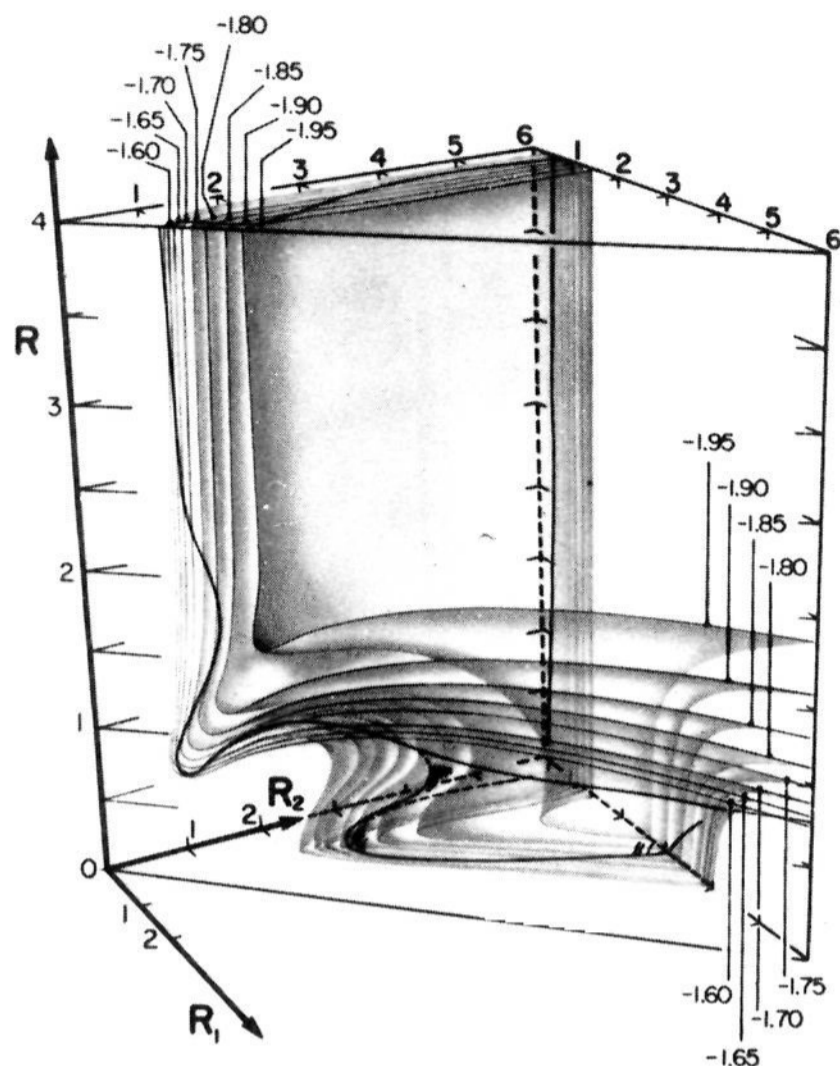


Figure 4. Equipotential surfaces of trapezoidal H_4 in the doubly excited (D) state.

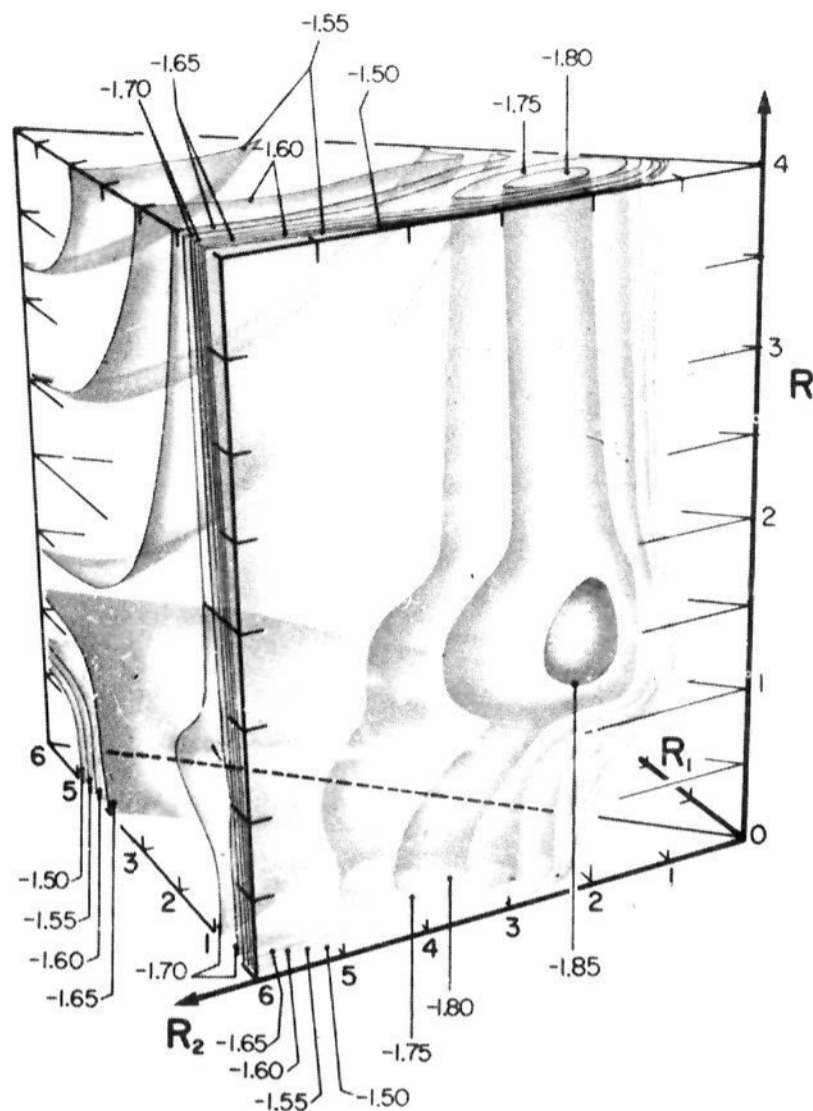


Figure 6. Equipotential surfaces of trapezoidal H_4 in the singly excited (S) state, viewed from the "rear".

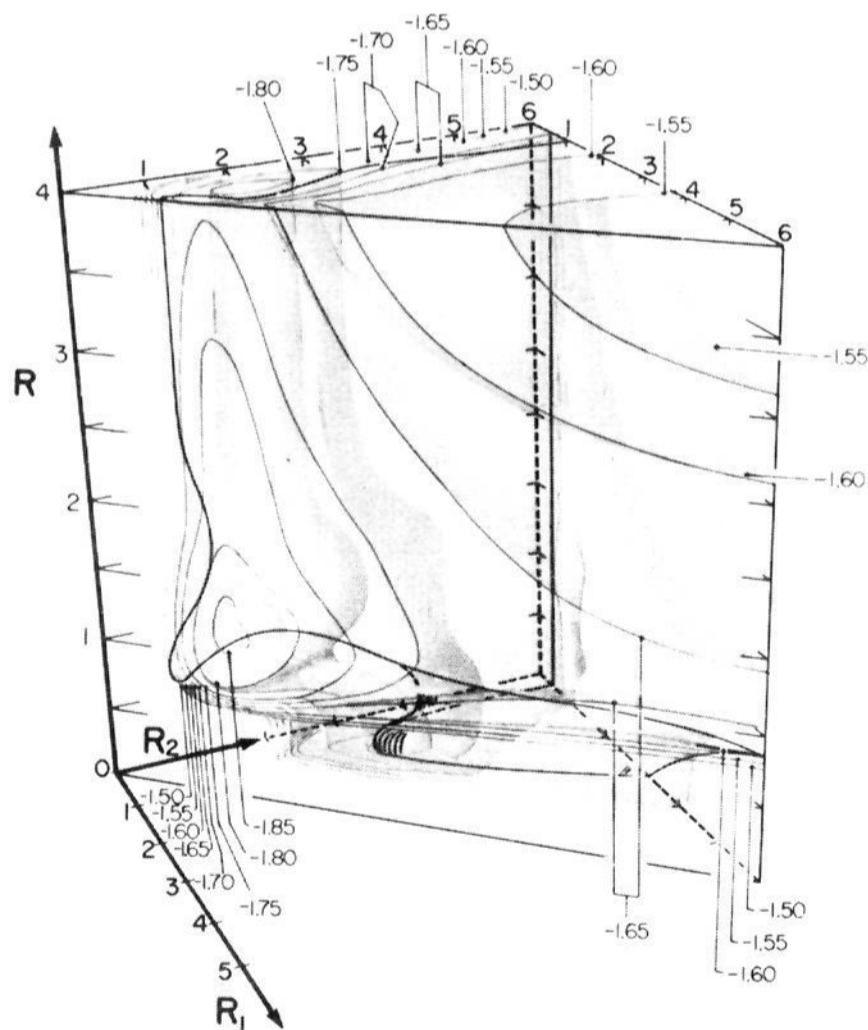


Figure 5. Equipotential surfaces of trapezoidal H_4 in the singly excited (S) state viewed from the "front".

since they are of no consequence for any of the following discussions, since the MB approximation is poor in this region so that our calculated results are undoubtedly grossly distorted, and since a finer grid of equipotential surfaces would be required.

The coordinate axes of Figures 2–6 are R_1 , R_2 , R , playing the roles of x , y , z in a right-handed Cartesian system. The scale for the vertical R axis is twice as large as for the R_1 and R_2 axes in order to improve visualization. In principle, all three coordinates range from $-\infty$ to $+\infty$. Since the energy is symmetrical across all coordinate axes, only one octant need be shown, namely the first: $R_1 \geq 0$, $R_2 \geq 0$, $R \geq 0$.

Certain lines and planes correspond to highly symmetrical special cases of the trapezoid. The plane $R_1 = R_2$ corresponds to all rectangular geometries, the line $R_1 = R_2 = R$ to all squares, and the plane $R = 0$ to all symmetrical linear geometries. The energy is unchanged when R_1 and R_2 are interchanged, $E(R_1, R_2, R) = E(R_2, R_1, R)$, so that the $R_1 = R_2$ plane divides the first octant into mirror image pairs. Hence it suffices to represent the energy surfaces on half of the first octant, $R_2 \geq R_1$ (the dark prism in Figure 7). A further symmetry exists in the plane of rectangles, namely reflection symmetry across the line of squares: $E(R_1, R_1, R) = E(R, R, R_1)$. The complete coordinate space, (R_1, R_2, R) , is shown in Figure 7. The coordinate planes $R_1 = 0$ and $R_2 = 0$ correspond to coincidences of two nuclei; no energy surfaces intersect these planes. The planes $R = 0$ and $R_1 = R_2$ are planes of mirror symmetry so that energy surfaces are normal to these planes (this is not always apparent in the figures). We further limit the surfaces by the planes $R = 4 \text{ \AA}$ and $R_2 = 6 \text{ \AA}$. At these large separations, the energy is changing slowly and extrapolation to infinity is allowed.

From Figure 1, note that changing the sign of R_1 interchanges nuclei A and B while that of R_2 interchanges C and D. Thus the first octant, $R_1 > 0$, $R_2 > 0$, $R > 0$, contains those trapezoids depicted in Figure 1. The second octant, $R_1 < 0$, $R_2 > 0$, $R > 0$, is unattainable via trapezoidal geometries since $R_1 = 0$ corresponds to infinite energy. This octant contains trapezoids in which A and B have been interchanged from the first octant. If the nuclei were distinguishable, these two octants would correspond to stereoisomers of one another. The third

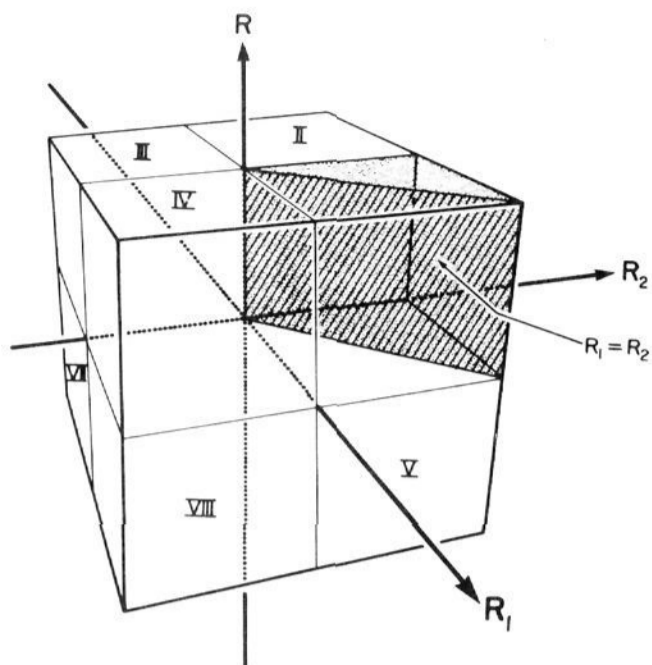


Figure 7. Complete coordinate space of trapezoidal H_4 .

octant, $R_1, R_2 < 0, R > 0$, corresponds to two interchanges or a pseudorotation from the first octant. The fourth octant $R_1, R > 0, R_2 < 0$, results from interchanging C and D from octant I or a pseudorotation from II. The fifth octant, $R_1, R_2 > 0, R < 0$, is attainable from I on paths which do not intersect $R_1 = R_2$ at $R = 0$. This octant corresponds to interchanging the parallel lines AB and CD from octant I and is equivalent to a pseudorotation. Similar relationships hold for all remaining octants.

In this way, the coordinate system depicted in Figures 2–6 contains all possible trapezoids in which the pairs AB and CD form parallel sides. Two other possibilities exist: the parallel sides formed by the pairs AC and BD or AD and BC. Because the nuclei are equivalent, these trapezoids produce energy surfaces identical with those of Figures 2–6 but with different definitions for the axes. The three sets of surfaces are conveniently distinguished by imagining them to be colored red, white, and blue, respectively. Namely, the red surfaces have $R_1 = \overline{AB}$, $R_2 = \overline{CD}$, and R the distance between parallel lines AB and CD as discussed above. The white surfaces have $R_1' = \overline{AC}$, $R_2' = \overline{BD}$, and R' the distance between parallel lines AC and BD. The blue surfaces have $R_1'' = \overline{AD}$, $R_2'' = \overline{BC}$, and R'' the distance between parallels AD and BC.

All three spaces have the origin in common. The red and white surfaces share the plane of rectangles in the first octant ($R_1 = R_2 = R', R_1' = R_2' = R$). The plane of rectangles in the second octant of the red surfaces is shared by the plane of rectangles in the fourth octant of the blue surfaces ($R_1 = -R_2 = R'', R_1'' = R_2'' = R$). Hence the three different colored surfaces mutually intersect. It is possible to pass smoothly from one set of colored surfaces to another set via their intersections at rectangular geometries. Since we will concentrate on the first octant of the red surfaces, we only discuss such transitions between red and white surfaces.

Imagine a rectangle $R_1 = R_2, R$ in the red surfaces. A distortion $R_1 < R_2$ leads to trapezoids in the red surfaces. But the plane of rectangles is shared by the white surfaces in which $R_1' = R_2' = R$ and $R' = R_1 = R_2$, so that a different distortion $R_1' < R_2'$ leads to white trapezoids. The shape of the white surfaces is derived from that of the red surfaces shown in Figures 2 to 6 by, first, rescaling the R axis by $2^{-1/2}$ (the line of squares, $R_1 = R_2 = R$, now bisects the right angle between the R axis and the $R_1 = R_2, R = 0$ line), second, relabeling the axes $R_1 \rightarrow R_1', R_2 \rightarrow R_2'$, and $R \rightarrow R'$, and third, rotating the entire space through 180° about the line of squares $R_1' = R_2' = R'$ so that the R' axis coincides with the former line $R_1 = R_2, R = 0$ and the line $R_1' = R_2', R = 0$ coincides with the former R axis. The same symmetry principles hold for red and white

(and blue) surfaces to allow each to be extended to all eight octants. Because of the symmetry within the $R_1 = R_2$ plane about the $R_1 = R_2 = R$ axis of rotation, the red contours and white contours coincide in this plane. Here the red and white surfaces join smoothly.

This simultaneous view of the two three-dimensional subspaces shows, for instance, that a point in the lower right corner in Figure 2 in the R_1, R_2, R subspace near the $R_1 = R_2$ plane is very close to a point in the upper left corner of the same figure but in the R_1', R_2', R' subspace and removes some of the perhaps otherwise puzzling lack of symmetry in the figures shown.

One additional point concerning the presentation of the results for the excited states S and D needs to be made. Either of these can be lower in energy, and since they are of different symmetries, they cross freely. The points at which the two surfaces have equal energy constitute a surface which is shown in Figures 4 and 5. Its cross section with the planes which limit the segment displayed is shown with a thick line (dashed where hidden from view). The shape of the surface within the segment is shown as it would appear in a perspective view, with a few shading lines but no continuous shading indicated to aid the reader. In the region between this cross-section surface and the R_1, R_2, R axes, the S state is below the D state in energy and represents the lowest excited singlet (S_1), in the rest of the space the D state is lower and represents S_1 .

The Ground State G (Figures 2 and 3). Our results for this state are of only secondary importance since better calculations have already been published,⁴ but a discussion is in order to introduce the use of three-dimensional contour maps on a case which is already reasonably familiar. Also, since the shape of our more approximate surfaces agrees quite closely with those obtained in ref 4, Figures 2 and 3 can be considered a condensed statement of what is presently known about ground state reaction paths in the trapezoidal subspace of the H_4 “molecule”.

Within the three-dimensional subspace R_1, R_2, R , the G hypersurface crosses no other surfaces and always represents the lowest singlet state S_0 . It touches the next higher singlet surface S_1 (D) asymptotically if R_1, R_2 , and R all go to infinity, since its energy then approaches that of four isolated H atoms (-2.0 au) from below, while the energy of the D state approaches this limit from above. This is indicated schematically in Figures 2 and 3, which contain a contour surface corresponding to energy -2.0 au in the upper right corner and in the front upper corner, respectively, although, strictly speaking, the -2.0 au limit is not reached until R_1, R_2 , and R and all infinite. This fictitious surface is drawn in to indicate the approximate region where the energy becomes virtually indistinguishable from -2.0 au.

The G surface is purely repulsive as far as interaction of two H_2 molecules is concerned, i.e., there is a downhill path from any point in the R_1, R_2, R subspace toward points representing two separated H_2 molecules in their $X^1\Sigma_g^+$ ground states. Possible very shallow minima of the van der Waals type¹² may be present but have not been sought; at any rate, they would not be discernible in Figures 2 and 3.

Square geometries are particularly energetic. The one of lowest energy (-2.0578 au) corresponds to a square of side 1.42 Å. Making the side of the square smaller than about 1 Å results in a rapid increase in energy, while making it longer than 1.42 Å requires relatively less energy and asymptotically approaches a square of infinite size at -2.0 au. If a square of any size is permitted to distort into a rectangle, the energy sooner or later decreases drastically as the molecule enters one of two “tubes” cut by the $R_1 = R_2$ plane. The first one is vertical in Figures 2 and 3 ($R_1 = R_2 = 0.76$ Å) and corresponds to a rectangle formed by two parallel molecules AB and CD. The other is horizontal in the figures ($R = 0.76$ Å) and cor-

Table II. Dimensions and Energies of Square, Trapezoidal, and Kite Forms of H_4 in the G, D, and S States as Computed by Various Methods^d

Geometry	Method	R^e	Energies, au				
			$-E_G$	$-E_D$	$-E_S$		
Square	MB	1.42	2.058*	1.952	1.851		
	MBP	1.42	2.058*	1.9525	1.853		
	<i>a</i>	1.31	2.075*	1.984	1.943		
	<i>b</i>	1.28	2.152*	2.042	2.076		
	<i>c</i>	1.16	2.065*	1.989	1.970		
	MB	1.27	2.051	1.935	1.861*		
	MBP	1.27	2.051	1.935	1.862*		
	EBP	1.15			1.9472*		
		R_1^f R_2^f R^f					
Trapezoid	MB	1.12	1.41	1.27	2.054	1.929	1.862*
	MBP	0.95	1.62	1.35	2.0818	1.9012	1.8685*
Kite		H_1^g H_2^g W^g					
	MB	0.33	1.43	1.84	2.0750	1.9018	1.8712*
	MBP	0.47	1.28	1.86	2.0686	1.9257	1.8792*

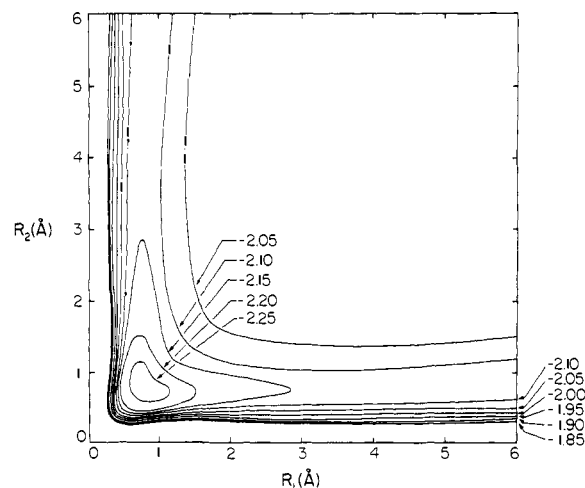
^a Reference 3a. ^b Results using Conroy's method including Monte Carlo integration, ref 3f. ^c Reference 3g; results using SCF-CI with 150 polarized terms. ^d The given dimensions are optimized for the state indicated by the asterisk. [All energies quoted are for nonlinear variation parameters optimized for the state cited]. ^e R = side of square in Å. ^f R = distance between parallel sides and R_1, R_2 = lengths of parallel sides in Å. ^g W = width of kite and H_1, H_2 = axial distance between vertices and cross axis in Å.

responds to a rectangle formed by two parallel molecules AC and BD. Within the $R_1 = R_2$ plane, the lowest energy path between the two "tubes" leads through the best square geometry, which lies about 148 kcal/mol above the calculated energy of two separated H_2 molecules. By comparison the best square of Rubinstein and Shavitt^{3a} has a side about 1.31 Å and lies 142 kcal/mol above two H_2 molecules. A summary of energies for H_4 in several states at the best square geometry, calculated by a variety of methods, is given in Table II. Distortion of the best square into one or the other rectangle brings at first a rapid decrease in energy; once the longer side of the rectangle is more than about 2 Å, however, further decrease in energy is only slow. The shape of the set of contour lines in the $R_1 = R_2$ plane is, of course, well known from elementary textbooks.

If a rectangle is allowed to distort into a trapezoid, the energy decreases further. This can be done in two ways: either AB and CD remain parallel (the red case) but are of unequal length, or AC and BD remain parallel but of unequal length (the white case).

The Red Case. This type of distortion of a rectangle occurs within the R_1, R_2, R subspace shown in Figures 2 and 3. Depending on which of the two parallel sides becomes longer, the point representing the geometry moves in front of or behind the $R_1 = R_2$ plane, and as has already been pointed out, the contour surfaces are perfectly symmetrical in both directions. We now need to describe the prominent features of the contour maps, namely the shape of the two tubes which have already been mentioned.

(i) **The Vertical Tube.** Since energy decreases as one moves a little away from the $R_1 = R_2$ plane, the tube actually has not one but two center lines, one on each side of the $R_1 = R_2$ plane, and these diverge further apart as R decreases. The cross section of the vertical tube is irregular, rather than circular, not only because of its double-pronged nature which becomes clearly pronounced in the region $R < 2$ Å (Figure 8 shows the cross section at $R = 2$ Å) but also because, for any value of R , it is much less costly in energy to increase only R_1 or only R_2

**Figure 8.** Cross section of the vertical tube in the ground state in the $R = 2$ Å plane.

rather than both simultaneously (i.e., to stretch only one rather than both parallel H_2 molecules). Once either R_1 or R_2 has increased beyond about 3 Å, the other being 0.76 Å, further increase requires very little additional energy (one of the two parallel H_2 molecules is dissociated into two H atoms, the other is at its equilibrium geometry). This provides a sideways escape from the vertical tube through a "joint", "crack", or "chimney", in rock climber's terminology, between the vertical contour surfaces which are partially hidden from view in the back of Figure 2 but are clearly seen on the right in Figure 3. For sufficiently large values of R_2 , these surfaces become exactly vertical (this is not clear from the drawings). Obviously, by reflection symmetry in the $R_1 = R_2$ plane, a similar escape through a crack is possible if R_2 is kept at 0.76 Å and R_1 increased beyond 3 Å (dissociation of the other of the two parallel H_2 molecules).

(ii) **The Horizontal Annular Tube.** The shape of this tube is considerably more complicated. It occurs at small values of R and large values of R_1 and R_2 , i.e., the energy is low because AC and BD form two hydrogen molecules of equal length, both in their ground state. For points inside the $R_1 = R_2$ plane, the two molecules are parallel since the four hydrogen atoms form a rectangle. For large values of R_1 and R_2 the energy minimum occurs at $R = 0.76$ Å. Moving in front of this plane or behind it again corresponds to making AB and CD unequal, i.e., keeping the two molecules AC and BD of equal lengths but rotating them in a disrotatory fashion about their respective centers (keeping all four atoms in a plane). Going behind the $R_1 = R_2$ plane in Figure 2 corresponds to bringing A and B closer together by such rotation; going in front of the plane brings the other ends of the two H_2 molecules closer together (C, D). In the other direction, rotation causes a decrease of the R coordinate and no change in the value of $R_1 + R_2$. Thus, the corresponding paths follow rings with centers on the line $R_1 = R_2, R = 0$, and lying in planes perpendicular to this line. When the amount of rotation in either direction becomes 90°, the $R = 0$ plane is reached, and the two H_2 molecules are collinear. If the motion in Figure 2 was behind the $R_1 = R_2$ plane, the order of the atoms on the line is C, A, B, and D, if it was in front of this plane, it is A, C, D, and B. For large values of R_1 and R_2 there will be negligible interaction between the AC and BD molecules, and the preferred length of both will be 0.76 Å. The points of lowest energy in the $R = 0$ plane will therefore lie on two lines, one on each side of the line $R_1 = R_2, R = 0$, parallel with it, for which $|R_2 - R_1|/2 = 0.76$ Å, i.e., separated from the $R_1 = R_2, R = 0$ line by about 1 Å. Either of the rotations can be continued to 180° by following the ring path below the $R = 0$ plane, and the point reached will again lie in

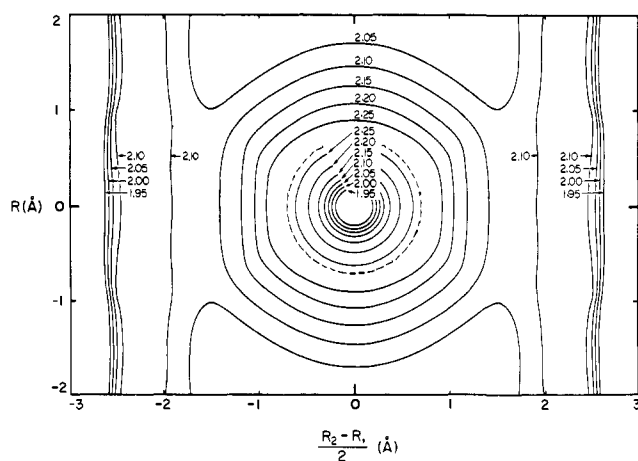


Figure 9. Cross section of the horizontal annular tube in the ground state in the $R_1 + R_2 = 6 \text{ \AA}$ plane.

the $R_1 = R_2$ plane and will be symmetrically disposed with respect to the starting point by mirroring in the $R = 0$ plane.

Thus, the shape to be expected of the contour surfaces defining the horizontal tube at large distance from the origin is that of a set of double-walled concentric cylinders whose axes coincide with the line $R_1 = R_2$, $R = 0$. A cross section of this tube at $R_1 + R_2 = 6$ is shown in Figure 9. Only one-quarter of each such cylinder is shown in the segment displayed in Figures 2 and 3. The "center" of the tube corresponds to a single-walled cylinder for which the length of the two molecules is 0.76 \AA (dashed line in Figure 9). The energy increases rapidly as one proceeds closer to the axis of the cylinders (shorter AC and BD) and reaches infinity on the axis itself. It also increases as one goes outward away from the axis, i.e., as the lengths of both H_2 molecules are increased.

As one proceeds down the horizontal tube toward the origin of coordinates, it gradually becomes clearer that all points on any given ring in a plane perpendicular to the line $R_1 = R_2$, $R = 0$ are not equally favorable. Once again, rectangles, i.e., points in the $R_1 = R_2$ plane, are relatively unfavorable, and energy is somewhat lower when the two H_2 molecules are not parallel. We have made no effort to ascertain which angle of rotation is best at which value of $(R_1 + R_2)/2$ (separation of the center of gravity of the two H_2 molecules), since this did not appear to be of particular importance and the accuracy of the MB procedure may not be sufficient. As the origin is approached, the two walls of the double-walled cylinders meet successively and the tube gradually comes to an end. A relatively easy escape is possible into the lower reaches of the "crack" described in connection with the vertical tube, but this is not clearly seen in Figure 3 because of the relatively coarse grid of potential hypersurfaces used. On the other hand, as the end of the horizontal tube is reached, motion toward the vertical tube requires a steeper climb in energy. The former "sideways" escape into the "crack" corresponding to an increase of R_2 corresponds to bringing the AC and BD molecules together, almost but not quite collinear, such that A comes within 0.76 \AA of B, while C and D fly off symmetrically in opposite directions. By symmetry, the same escape possibility is repeated four times around the horizontal tube (Figure 9). The escape proceeds uphill in energy until a point near $R_2 = 4.8 \text{ \AA}$ is reached; thereafter it proceeds slightly downhill. Thus, a sideways entrance into the horizontal tube encounters a small activation energy (about 4 kcal/mol).

The White Case. The other type of distortion from a rectangular geometry, in which AC and BD remain parallel but of unequal lengths, leads to the white R_1', R_2', R' subspace. Recalling our previous discussion of how this subspace is at-

tached to the red R_1, R_2, R subspace, sharing the $R_1 = R_2$ plane, but being rotated so that the direction of R' axis coincides with the line $R_1 = R_2$, $R = 0$, while the direction of the line $R_1' = R_2'$, $R' = 0$ coincides with the R axis, we note that entry into the R_1', R_2', R' subspace from any of the points located where the red vertical tube cuts the $R_1 = R_2$ plane will lead into an area of white contour surfaces which have the same shapes as the red horizontal tube does in Figures 2 and 3. Similarly, entry into the R_1', R_2', R' subspace from any of the points located where the red horizontal tube cuts the $R_1 = R_2$ plane will lead to an area of white surfaces whose shapes look just like those of the red vertical tube in Figures 2 and 3. Thus, no further description is necessary beyond noting that a point moving in the $R_1 = R_2$ plane down the vertical tube and one moving in the same plane along the horizontal tube "see" the same three-dimensional contour surfaces surrounding them, i.e., red and white simultaneously.

This situation, in which a set of contour lines in a plane, in our case the $R_1 = R_2$ plane, can be equally well continued into the third dimension on either side by one or another set of contour surfaces, which we chose to distinguish by color, is a direct consequence of the multidimensionality of the nuclear configuration space. A representation of a four-dimensional contour map could be similarly provided by use of an infinite number of color shades, just as a representation of a three-dimensional contour map could be provided by an infinite set of differently colored two-dimensional contour maps all of which share one common line (each color corresponding to cross sections of the three-dimensional contour surfaces with one possible plane containing the line). In our case, contour surfaces in additional colors could be used to represent additional three-dimensional subspaces which share the two-dimensional subspace of all rectangles with the R_1, R_2, R and R_1', R_2', R' subspaces, but we presently have no results for these. It appears important to obtain them in the future, since, as we noted above, in both the vertical and the horizontal tube, deviation from rectangular geometries is advantageous and is achieved by allowing the two H_2 molecules to have unequal length in the former case and allowing them not to be parallel in the latter. It is highly probable that simultaneous relaxation of both conditions, leading outside both the R_1, R_2, R and R_1', R_2', R' subspaces, would lead to even lower energies.

It is already clear from previous work⁴ that the $\text{H}_2 + \text{D}_2$ isotopic exchange reaction, if it occurs as a simple bimolecular exchange process at all, does not proceed through the R_1, R_2, R (or R_1', R_2', R') subspace. This reaction involves a path which starts in one of the two tubes and ends in the other. Within the trapezoidal subspaces, an H_4 system entering either tube with energy -2.15 au or less, i.e., with energies up to at least 90 kcal/mol above the sum of energies of two ground state H_2 molecules, can find no way to escape from the tube, and eventually separates into the two initial H_2 molecules. If more energy is available, one of the two H_2 molecules can dissociate, and this corresponds to escape from the vertical tube through the crack described above (i.e., escape from the red vertical tube or white horizontal tube, which has the same shape). Alternatively, two atoms, one in each H_2 molecule, which were originally not mutually bonded, can approach and form a new bond, losing their old bonding partners to infinity in opposite directions, and this corresponds to a reaction $\text{H}_2 + \text{D}_2 \rightarrow \text{HD} + \text{H} + \text{D}$ proceeding by the "sideways" escape from the horizontal tube toward the right in Figure 3 as discussed above (i.e., escape from the red horizontal or white vertical tube). Our calculations are not sufficiently reliable to tell whether it will take even more energy to proceed from one tube to the other, but the more detailed results of previous authors^{4a} indicate that it will, by 6 kcal/mol . The path suggested by them is similar to what one would expect from Figure 3, i.e., proceeds via the sideways escape from the horizontal tube. Figure 3 also indi-

cates quite strongly, but does not prove, that the processes leading to dissociation of one of the H_2 molecules will start to occur at lower energies than the $H_2 + D_2 \rightleftharpoons 2HD$ exchange and makes it clear that the best paths for such exchange avoid rectangular geometries. As mentioned above, we consider it very likely that they also avoid trapezoidal geometries, and that the reaction path suggested in ref 4a is not followed in reality (the mechanism may be termolecular^{4b}).

The Doubly Excited State D (Figure 4). The region of very high energies for the G state near the line of the square geometries ($R_1 = R_2 = R$) originates in an avoided touching with another state of A_1 symmetry in the C_{2v} group, which we refer to as D, for doubly excited. The same avoided touching causes a region of low energies for the D state near the line of square geometries, clearly apparent in Figure 4. The separation of the two states is about 3 eV for the best ground state square ($1.42 \times 1.42 \text{ \AA}$), increases rapidly as the size of the square decreases, and approaches zero asymptotically in the limit $R_1 \rightarrow \infty$, $R_2 \rightarrow \infty$, $R \rightarrow \infty$, where the energy of the D state approaches -2.0 au from above. The region in which the energy becomes virtually exactly -2.0 au is approximately the same as for the G state and is not shown explicitly (cf. Figures 2 and 3).

The D state is purely repulsive; i.e., there is a downhill path from any point in the R_1, R_2, R subspace leading to four separated ground state H atoms. The surface is repulsive for each of the two H_2 molecules separately and also as far as their trapezoidal approach is concerned. In either limit of separated H_2 molecules, i.e., large R and small R_1 and R_2 or large R_1 and R_2 and small R , it correlates with two H_2 molecules in their purely repulsive $b^3\Sigma_u^+$ triplet states. The uphill path of least resistance follows square geometries. It takes about 50 kcal/mol to reach a $1.25 \times 1.25 \text{ \AA}$ square, and the energy rises quite rapidly afterwards. The "bay" of low energies found at the small square geometries can be understood as resulting from increasing efficiency with which the touching between the G and D states is avoided as the overlap of the atomic orbitals increases; eventually, of course, nuclear repulsion takes over and the bay ends.

Similarly as shown for the G state, the contour surfaces of the D state in the R_1, R_2, R subspace also define those for the R_1', R_2', R' subspace, and one can imagine two colored sets of surfaces in the region $R \geq 0$, $R_1 \geq 0$, $R_2 \geq 0$ sharing a common $R_1 = R_2$ plane.

The Singly Excited State S (Figures 5 and 6). Of the three states considered here, the S state is the only one which contains an energy minimum for a significantly bound H_4 species. It correlates with one ground state $X^1\Sigma_g^+$ hydrogen molecule and one $B^1\Sigma_u^+$ singly excited hydrogen molecule located parallel to each other. In the limit of four separated hydrogen atoms, it correlates with $H + H + H^+ + H^-$ (incorrectly, since Rydberg states are excluded from our minimum basis set calculation). There is a downhill path from any point in the R_1, R_2, R subspace toward the minimum, located at a trapezoidal geometry (two parallel H_2 molecules of lengths $R_1 = 1.12 \text{ \AA}$ and $R_2 = 1.41 \text{ \AA}$ separated by $R = 1.27 \text{ \AA}$). The minimum lies inside an egg-shaped closed surface in the lower left corner of Figure 5, and its energy is -1.862 au . In the $R_1 = R_2$ plane, the energy is lowest at the geometry of a $1.27 \times 1.27 \text{ \AA}$ square (-1.861 au). In this plane, two paths lead to this geometry, a vertical one representing a combination of parallel AC and BD molecules and a horizontal one representing a combination of parallel AC and BD molecular. If a rectangle or a square is allowed to distort into a trapezoid, its energy decreases. Again, we need to distinguish the red case (AB and CD parallel but of unequal lengths) and the white case (AC and BD parallel but of unequal lengths). The red case corresponds to distortions within the R_1, R_2, R subspace, so that red surfaces and coordinates are applicable (those shown in Figures

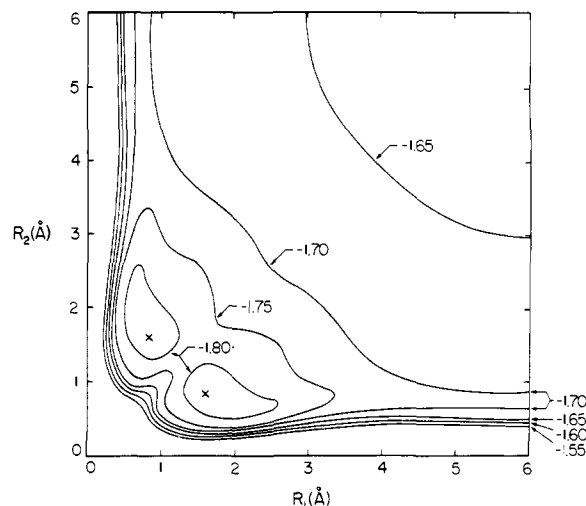


Figure 10. Cross section of the twin vertical tubes in the singly excited state in the $R = 2 \text{ \AA}$ plane.

5 and 6); the white case corresponds to distortions within the R_1', R_2', R' subspace, so that white surfaces and coordinates are applicable (those obtained from the red set by the previously described procedures).

The Red Case. Although the horizontal and vertical paths leading to the best square minimum in the $R_1 = R_2$ plane are identical because of symmetry across the line of squares, their surroundings behind (or in front) the plane are greatly different (Figures 5 and 6).

(i) **The Vertical Path.** This corresponds to an approach of two parallel hydrogen molecules, one long (1.84 \AA), in its $B^1\Sigma_u^+$ excited singlet state, the other short (0.76 \AA), in its $X^1\Sigma_g^+$ ground state. This path appears as a vertical tube in the figures; by symmetry with respect to the $R_1 = R_2$ plane, two such tubes are actually present (four if one also considers the region $R < 0$ and 16 if one also considers $R_1 < 0$ and $R_2 < 0$). The center lines of the two tubes approach each other toward the bottom but do not meet; each ends in a separate trapezoid minimum, one on each side of the $R_1 = R_2$ plane. Since our calculation overestimates the equilibrium length of the H_2 molecule in its $B^1\Sigma_u^+$ state, there is no doubt that it also overestimates the distance from the $R_1 = R_2$ plane to the center lines of the tubes. The descent in energy down the center of the tube is relatively mild, from -1.820 au at $R = \infty$ to -1.862 au at the minimum ($\Delta H = -26 \text{ kcal/mol}$). Once the minimum is reached, further decrease in R causes rapid increase in energy.

The cross section of each tube in a direction perpendicular to its center line is unsymmetrical (Figure 10), since it is easier to stretch the one H_2 molecule which is already long and excited (CD) than it is to stretch the other (AB). Once the longer H_2 molecule has been stretched beyond about 3 \AA , the other being 0.76 \AA , further increase in R_2 requires little additional energy. In this way, H_4 can dissociate to a ground state H_2 molecule, H^+ , and H^- (in better calculation, a Rydberg state would intervene at this point and provide for dissociation into a ground state H atom and an excited H atom). This process corresponds to a sideways escape from the vertical funnel through a "crack" between the vertical contour surfaces which are clearly seen in Figure 6. For sufficiently large values of R_2 , these become strictly vertical. By symmetry, a similar crack adjoins the other vertical tube and corresponds to dissociation of the other hydrogen molecule (AB).

Motion of a point between the two vertical tubes becomes easier as the value of R decreases. To go from one of the end minima to the other, a barrier of only 0.5 kcal/mol needs to be surmounted (the path of least energy leads through the best square). The cross section through the minima and perpen-

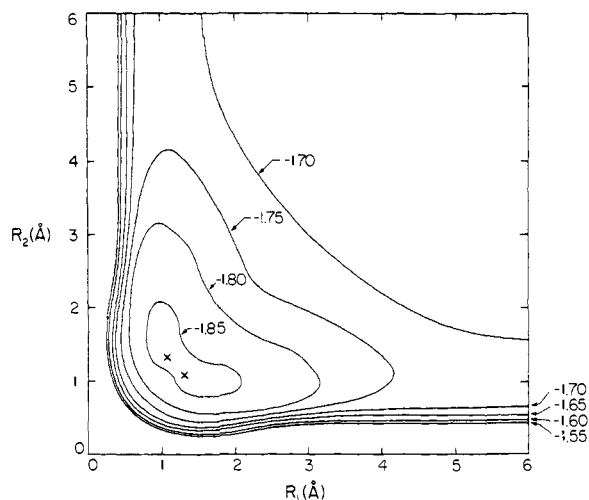


Figure 11. Cross section of the vertical tube in the singly excited state passing through the minima in the $R = 1.2 \text{ \AA}$ plane.

dicular to R is shown in Figure 11. The barrier is accentuated with a calculation at the MBP level (4 kcal/mol).

(ii) **The Horizontal Path.** Moving out of the $R_1 = R_2$ plane in the region where R is small (1–1.5 Å) and R_1 and R_2 large corresponds to rotating the two H_2 molecules AC and BD out of parallelity but keeping them of equal lengths. This corresponds to only a small decrease in energy, even if the angle of rotation is large. There is no tube of low energy on either side of the $R_1 = R_2$ plane. This is easy to understand, since such a tube would correspond to an approach of two H_2 molecules, AC and BD, but in this region of the R_1, R_2, R subspace, both are compelled to be of equal lengths, which is a high-energy situation. Being able to localize the electronic excitation on one of the two molecules by stretching it, such as was the case for the vertical tube, would provide the path to lower energies.

The White Case. Going from the $R_1 = R_2$ plane into the subspace R_1', R_2', R' of white surfaces instead of the above-described R_1, R_2, R subspace of red surfaces again interchanges the horizontal and vertical directions. The two white tubes are horizontal, containing geometries at which the molecules AC and BD are parallel but have unequal lengths, while no well-developed white vertical tubes exist (the two molecules are forced to have equal lengths).

In summary, there are four trapezoidal minima in the region $R \geq 0, R_1, R_2 \geq 0$ ($R' > 0, R_1', R_2' \geq 0$), two formed by red surfaces (AB longer or shorter than CD and parallel to it) and two by white surfaces (AC longer or shorter than BD and parallel to it). Vertical tubes lead from above into each of the red minima and horizontal tubes lead into each of the white minima. Motion from any one of the four minima into any of the others is easy and proceeds through the best square geometry.

Entering through one of the four tubes and leaving through the same one corresponds to no chemical change, leaving through the other tube of the same color corresponds to excitation energy transfer, leaving through one of the two tubes of the other color corresponds to an adiabatic exchange reaction of the type $\text{H}_2 + \text{D}_2 \rightarrow 2\text{HD}$, leaving excitation on one or the other product molecule.

An additional reaction path of relatively low energy exists and is clearly seen both in Figures 5 and 6. This follows a tube which joins the region of the trapezoidal minimum with the plane of linear geometries, $R = 0$. By symmetry, it continues below the $R = 0$ plane and reaches a trapezoidal minimum located symmetrically to the one at the start. It is then possible to close a loop, of which only one quarter is displayed in Figures 5 and 6, by proceeding to the front of the $R_1 = R_2$ plane and up, through the $R = 0$ plane again, and back to the starting

point through the $R_1 = R_2$ plane. A similar loop exists in the white surfaces.

Physically, motion along the loop corresponds to squashing a “best” trapezoid ABCD from the top until the atoms lie all in one line, CABD, during which process R_2 , i.e., \overline{CD} , increases considerably, and continuing this motion, now with AB on the other side of CD, bringing CD closer together again until the best trapezoidal geometry is reached, equalizing sides to a square, then making AB longer than CD and now pushing CD through AB similarly as above, going through a linear arrangement ACBD, continuing to the “best trapezoid” with AB now on the original side of CD, changing to a square and finally making AB shorter again and CD longer to return to the starting point. In addition to being viewed as mutual penetration of two parallel H_2 molecules, this process can also be considered as simultaneous disrotatory motion of two opposite sides of a square. At either of the two square geometries ($R > 0$ and $R < 0$), a choice exists to enter a similar loop in the white surfaces, corresponding to the rotation of the other pair of opposite sides of the square.

We have made no attempt to locate the transition states in this process or to calculate its energy since minimum basis set calculations for the S state can only be considered semiquantitative. They must be located in the $R = 0$ plane (if no intermediates are present). However, since all of the loop is calculated at relatively low energies (–1.80 au and less) we are quite confident about its existence and general shape.

As is clear from Figures 4 and 5, throughout most of the R_1, R_2, R space the D state is below S in energy. Only if one or both pairs of H atoms are close together is the order reversed. The location of the crossing surface separating the two regions of the R_1, R_2, R space is calculated only approximately, since one of the states (D) is predominantly covalent while the other (S) is ionic and therefore undoubtedly calculated with larger error. For this reason, no very serious attempt was made to draw the crossing surface exactly in the figures. Its general shape as indicated is probably quite correct, but it ought to lie somewhat farther away from the coordinate axes. Calculations with a 1s 2s basis set still predict that D is below S in the region of the minimum. In order to settle the order of D and S states and find points of their mutual crossing along reaction paths corresponding to the various tubes in Figures 4 and 5, extended basis set calculations would again be necessary. These have not been performed for this initial study. Clearly, overall trends are the only result which can be extrapolated from H_4 to $2s + 2s$ reactions in general (relative state energies and details of geometries of crossing will vary from molecule to molecule, but general principles of bonding and antibonding interactions which define the gross shapes of surfaces will most likely remain the same).

G, D, and S States. Other than Trapezoidal Geometries.

Although the present study concentrates on the trapezoidal geometries of H_4 , two remarks concerning our results for other geometries will aid the following discussion. First, we note that the trapezoidal minimum in the S surface is not a minimum within the total six-dimensional space, since a distortion to a kitelike shape of C_{2v} symmetry lowers the energy by 7 kcal/mol (MBP). A more detailed study of the properties of the H_4 excimer will be published separately. Whether extended basis set calculations will show the same equilibrium geometry for the excimer is not yet known. The lowest energy thus far obtained for the S state is –1.9521 au for a trapezoidal geometry (EBP). Fine details, such as the precise equilibrium geometry of the excimer, may change in a better calculation, but the qualitative description of potential surfaces surely will not change.

Second, while the steepest descent from a $1.27 \times 1.27 \text{ \AA}$ or similar square on the D surface within the R_1, R_2, R (or R_1', R_2', R') surface corresponds to an increase of the size of

the square, this is not the direction of steepest descent when the whole six-dimensional space is considered. Energy decreases even faster upon distortion into a rhombus, achieved by a diagonal motion of two hydrogen atoms at opposite corners of the square toward the center, and by simultaneous diagonal motion of the other two away from the center. This path leads to the formation of a ground state hydrogen molecule from the two atoms moving toward each other and removal of the other two atoms to infinity. During this process, the D state decreases in energy rapidly, crosses the G state which rises, and becomes the lowest singlet state S_0 . An even larger energy gain is possible if the two departing hydrogen atoms are not permitted to go to infinity but instead both are brought above the original plane of the square and allowed to approach to a mutual distance of 0.76 Å, thus forming a second ground state H_2 molecule (the G and D states are degenerate at tetrahedral geometries). These processes, involving formation of covalent bonds along one or both diagonals of the original square, are easily understood in light of the following discussion of the nature of bonding in the G and D states in VB terms. A more detailed discussion of our results for the corresponding additional subspaces of the nuclear configuration space of H_4 will be presented elsewhere.

Discussion

G, D, and S States. Wave Functions. Electronic States at a Biradicaloid Geometry. We shall first provide a simple description of the calculated wave functions at rectangular geometries ($R_1 = R_2$), needed for a subsequent general discussion of $2s + 2s$ processes. The wave functions at nearby trapezoidal geometries are not very different and similar considerations apply. Larger changes occur as the geometry is distorted to linear ($R = 0$) and this will be discussed subsequently.

Rectangular Geometries. In the simple molecular orbital (MO) picture (see, e.g., ref 13), the G state is represented by the ground configuration ψ_0 (the lowest two of the four MO's doubly occupied), the S state by a singly excited configuration $\psi_{1 \rightarrow -1}$ [one electron promoted from the highest occupied MO (HOMO) to the lowest unoccupied MO (LUMO)], the D state by a doubly excited configuration $\psi_{1,1 \rightarrow -1,-1}$ (both electrons promoted from HOMO to LUMO) mixed with excited configurations involving also the other two of the total four MO's. This description is reasonably adequate if the gap between HOMO and LUMO is large, i.e., in the regions of space corresponding to two short H_2 molecules relatively far apart (narrow and long rectangle). As is well known from orbital symmetry arguments,⁵ HOMO and LUMO change place if the line $R_1 = R_2 = R$ (squares) is crossed; at square geometries, they are nonbonding and degenerate by symmetry, and since they contain, in low-lying states, a total of only two electrons, the geometry can be called "biradicaloid".^{14,15} As a square geometry is approached, the simple description of G as ψ_0 and D as $\psi_{1,1 \rightarrow -1,-1}$ mixed with a few other excited configurations becomes unacceptable, since ψ_0 and $\psi_{1,1 \rightarrow -1,-1}$ begin to mix strongly. At square geometries the G state is described as $\psi_0 - \psi_{1,1 \rightarrow -1,-1}$, the S state as $\psi_{1 \rightarrow -1}$, and the D state as $\psi_0 + \psi_{1,1 \rightarrow -1,-1}$ with sizable admixture of other excited configurations. Thus, as HOMO and LUMO exchange places upon going across the line of all squares, the G and D states undergo an avoided crossing.

In the simplest MO description of a species at a biradicaloid geometry,^{14,16} only the three lowest energy configurations are allowed to mix, ψ_0 , $\psi_{1 \rightarrow -1}$, and $\psi_{1,1 \rightarrow -1,-1}$. This 3×3 CI has been used in some calculations of reaction paths for organic molecules,¹⁷ and if only the ground state is of interest, only ψ_0 and $\psi_{1,1 \rightarrow -1,-1}$ are sometimes used.¹⁸ In the 3×3 CI scheme, the calculated order of excited states is invariably G lowest, S higher, and D highest, and their energy differences can be

written explicitly in terms of integrals over MO's. Expansion of the 3×3 CI wave functions in terms of AO's shows that the G state is purely covalent and the D and S states purely ionic (zwitterionic).^{14,16}

For H_4 squares, we find this order only if the side of the square is quite small (< ca. 0.75 Å), and we find the order G, D, S for all squares of interest for reaction paths. Even if we consider the differential error introduced into the ionic S state by use of a minimum basis set, there is no doubt that the G, D, S order applies for most squares. In MO terms, the lowering of the D state below the S state is due to mixing with other configuration which also involve orbitals other than HOMO and LUMO, and which are not considered in the simple 3×3 CI procedure. This mixing is much more important for the D state than the S state, as has been also noted for other biradicaloid species.¹⁹ A simple physical reason for this striking difference is provided by a VB analysis of the bonding situation. At any rate, it seems obvious that a simple 3×3 CI description of molecules at biradicaloid geometries, although it predicts the correct number of low-lying excited states, cannot be used to deduce the order of the D and S states.

In the simple VB description, the G and D states are covalent and the S state is ionic. At rectangular geometries for which $R_1 = R_2 < R$, the G state is best described by singlet pairing (bonds) between A and B and between C and D, with a minor contribution from a structure in which A is bonded to C and B to D by "long" bonds, while in the D state the structure with long bonds dominates and the one with short bonds is minor. As a square geometry is approached, the contributions of the two structures become equal. Thus, the avoided crossing is between the VB structure $\psi_{AB,CD}$ and the VB structure $\psi_{AC,BD}$.

The simple VB description of the S state is more difficult since its wave function contains a large number of singly and even doubly ionic structures, mostly of the type $A-B, C^+D^-$, and those related by symmetry. In order to see why one of the numerous ionic states is of particularly low energy, it is best to consider its parentage in a $X^1\Sigma_g^+$ ground state H_2 molecule, represented simply as $A-B$, and a $B^1\Sigma_u^+$ singly excited H_2 molecule, represented simply as $C^+D^- \leftrightarrow C^-D^+$ (out-of-phase combination; the in-phase combination corresponds to the higher energy doubly excited $E^1\Sigma_g^+$ state). In the $R_1 = R_2$ plane, and at infinite intermolecular separations, the S state is degenerate, since representations $A-B, C^+D^- \leftrightarrow A-B, C^-D^+$ and $A^+B^-, C-D \leftrightarrow A^-B^+, C-D$ are equal in energy and noninteracting. As the molecules approach, the originally degenerate components interact, one decreasing in energy (S), the other increasing. These, of course, are the two well-known exciton states. If the approach of the two molecules occurs outside the $R_1 = R_2$ plane, i.e., at a trapezoidal geometry, the degeneracy is absent even at infinite separations, the excitation is predominantly localized on the longer of the two molecules, the energy is lower (the center of the vertical tube in Figures 4 and 5 lies behind the $R_1 = R_2$ plane), and the exciton splitting is less. As the two H_2 molecules in the S state approach even closer, another class of ionic structures decreases in energy and they start to contribute significantly to the wave function of the S state. These are charge-transfer structures of the type $A^+ B-C D^-, A^+ B-D C^-,$ etc. This interaction causes further stabilization of the S state, maximized when a square geometry is reached. The downhill slope of the S surface is thus attributed to a combination of exciton interaction and charge-transfer interaction, exactly the two factors which are believed to be responsible for the stability of excimers and exciplexes in general.²⁰ The H_4 excimer appears to represent an optimum case for excimer formation because of its high symmetry and because all electrons present participate in the two stabilizing factors. On the other hand most known excimers involve large π -electron organic molecules whose σ framework constitutes

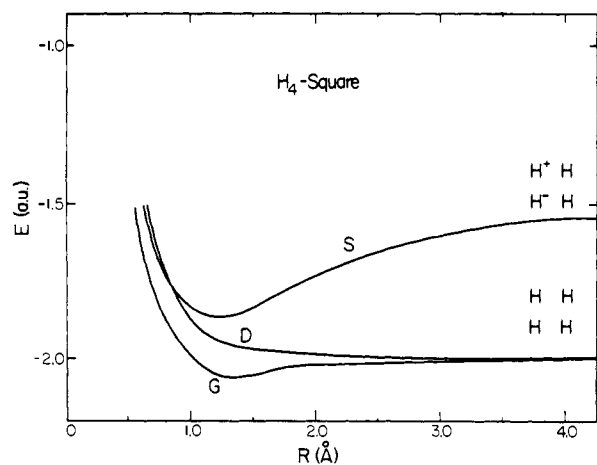


Figure 12. The three lowest electronic states of H_4 at square geometries ($R = R_1 = R_2$).

closed shells which resist intimate approach of the components.

Thus, at square geometries the simple VB picture suggests the presence of two low-lying covalent states G and D and a variety of ionic states, of which one (S) should be considerably lower than most others. It predicts an energy ordering G, D, S, at least at those geometries (large squares) in which interactions between the four centers are relatively weak, charge separation costly, and state energies determined mostly by structure energies, which are of course lower if no charge separation is involved. This is in better agreement with the actual ordering at geometries of practical interest, G, D, S, than the simple MO view. Both simple views agree that the G state is covalent and the S state ionic, but they disagree on the nature of the D state. As could be expected in such an instance, the full CI answer is in between: the D state contains both covalent and ionic contributions. If one starts from the simplest VB standpoint which would describe both the G and D state as superpositions of the two covalent VB structures, going to full CI involves much heavier mixing of the D state than of the G state with additional ionic structures. If one starts from the simplest MO standpoint which would describe both the D and S states as ionic ($\psi_0 + \psi_{1,1} \rightarrow -1, -1$, and $\psi_{1,-1}$, respectively), going to full CI involves much heavier mixing of the D state than the S state with additional configurations, which has the effect of decreasing its ionic nature. This substantial mixing was already noted above and the just presented VB viewpoint helps us understand why it occurs. As the mixing decreases the otherwise highly ionic nature of the wave function, it also lowers the energy of the D state, quite possibly below that of the S state.

Whether the full CI answer lies closer to one or the other extreme, simple MO or simple VB, depends on the strength of interatomic interactions, or coupling (Figure 12). For weak coupling (large squares), the full CI solution is quite close to the simple VB picture. In the limit of an infinite square, the D state is indeed purely covalent and degenerate with the G state, both corresponding to four neutral separated hydrogen atoms (four doublets can be coupled into a singlet in two linearly independent ways). The S state is much higher and is degenerate with several other ionic states. For strong coupling (small squares), the full CI solution is quite close to the simple MO picture and the D state is quite ionic and high above the S state in energy. The situation is, of course, similar as in diatomic molecules, where the simple MO description only works for small interatomic separations. Perhaps not surprisingly, the size of squares of most interest for discussion of reaction paths is such that neither simple description applies.

The covalent, or partly covalent, nature of the D state is also

apparent from its parentage in two (covalent) triplet H_2 molecules lying side by side, analogous to the parentage of the G state in two (covalent) singlet H_2 molecules lying side by side. As an H_4 molecule in its D (G) state is distorted from a square geometry to a rectangular one, antibonding (bonding) local triplet (singlet) character appears along the shorter pair of H-H distances. Inspection of the spin coupling scheme also shows that the diagonal interactions in the D state become bonding (local singlet) and in the G state antibonding (local triplet) if one or both diagonals are shortened by distortion toward a rhombus or a tetrahedron. Thus, the square H_4 molecule in its D (G) state also correlates with two singlet (triplet) H_2 molecules laid out diagonally across each other. This provides a simple rationalization of the downhill paths noted above for the D surface and may provide a clue in the search for the mechanism of the $H_2 + D_2$ exchange reaction in the ground state.

Linear Geometries. Similarly as in the case of rectangular geometries, a surface of avoided touching between the G and D states separates the region of the horizontal tube (R_1 and R_2 both large) from the region of the vertical chimney ($R_1 \approx 0.76 \text{ \AA}$, $R_2 > 3 \text{ \AA}$). It goes through the point of high energy on the "sideways escape" path from the horizontal tube (Figure 3). For points in the horizontal tube, the prevailing VB coupling scheme is C-A, B-D in the G state, with a minor contribution from A-B, C-D, just as it was for rectangular geometries. This is not surprising since for large R_1 and R_2 travel around the rings from rectangular to linear geometries corresponds to rotation of two almost noninteracting H_2 molecules. In the D state, A-B, C-D coupling prevails at these geometries and C-A, B-D is minor. For points in the vertical crack lying beyond the point of escape, the opposite is true, and thus the two parts of space corresponding to the two different coupling schemes are approximately separated by a surface which contains the line of all squares and cuts the plane of linear geometries ($R = 0$) in a curved line which starts near the origin and proceeds approximately toward the point $R_1 = 2 \text{ \AA}$, $R_2 = 6 \text{ \AA}$. In between the two lines, the surface follows the series of deep furrows which represent relatively high energies for the G state (Figure 3) and relatively low energies for the D state. Obviously, the very existence of these conspicuous furrows is due to the avoided touching.

Along the points near the "sideways escape" from the horizontal tube, ground state H_4 can be described as a "loose biradicaloid"¹⁴ C-A-B-D as opposed to the "tight biradicaloid" at square geometries. Up to a point along this path it is cheapest in energy to break the already partially established A-B bond and return to C-A + B-D so that the species is still best viewed as $2H_2$. Beyond this point, which corresponds to the avoided crossing of the two VB structures, the downhill path is for the two "radical centers" C and D to wander off to infinity, so that the species can be best viewed as $H + H_2 + H$. Once on the other side of the surface of avoided crossing, the centers B and D can join to make a second bond (C-D) without further activation energy by moving toward the vertical tube, but the path toward it is extremely flat (cf. the twixtyl concept of Hoffmann et al.²¹). The stepwise character of a symmetry forbidden ground state reaction is thus clearly apparent; the activation barrier occurs as the new bond (A-B) is made and the old bonds (C-A and B-D) broken, after which a period of search follows in which the two loose ends (C and D) grope for each other (cf. ref 21).

The wave function for the D state contains again considerable ionic character. In this state, the energy is lowest when H_4 dissociates into 4 H atoms, but if the atoms were forced to stay together, it would cost least energy to adopt one of the geometries corresponding to the surface of avoided crossings, and among those "tight" geometries (square) are better than "loose" ones (linear) in accordance with qualitative argu-

ments¹⁴ based on the presence of ionic character in the D wave function.

The wave function for the S state is purely ionic and similar to that discussed for rectangular geometries. The tendency for points of low energy to occur at relatively short internuclear distances is even more pronounced than it was for the D state, again in agreement with qualitative notions based on ionic character.

Photochemical Processes in H₄. Little seems to be known experimentally about bimolecular photochemistry of the H₂ molecule. The fluorescence of excited HD ($B^1\Sigma_u^+$) is effectively quenched by H₂ or D₂. Electronic energy transfer to the quencher is inefficient; the nature of the other processes involved is, however, unknown.^{2b} Our study of low-lying singlet surfaces for trapezoidal geometries suggests certain possibilities, but we hesitate to draw many definite conclusions, both because only such a small region of the total six-dimensional hyperspace has been explored so far, and because our method of calculation provides no information about Rydberg excited states which in H₂ do not lie very high above the valence excited states. Also, as already noted, results on mutual separation of the covalent D state and the ionic S state are only semiquantitative in nature. In the following, we shall outline some of the possibilities suggested by our calculations for an encounter of a ground state $X^1\Sigma_g^+$ H₂ molecule with a singlet excited $B^1\Sigma_u^+$ H₂ molecule.

A result which we feel is beyond doubt is formation of a bound H₄ excimer in an adiabatic process. At the MBP level, the minimum energy geometry of this species lies outside the three-dimensional subspace explored here, as already mentioned. The best trapezoid (parallel sides of length 1.62 and 0.95 Å located 1.35 Å apart) is not much higher in energy (7 kcal/mol), nor is the best rectangle, which is a square 1.27×1.27 Å in size (another 4 kcal/mol higher). These details may change at the EBP level. A variety of automerization processes appears possible for the excimer, in which it reaches square, trapezoidal, kite, linear, and probably other geometries as its sides exchange their lengths (pseudorotation), rotate with respect to each other, etc. The excimer can also separate into two H₂ molecules, with various possibilities for atom exchange in the overall process. A detailed study of these possibilities will require use of a larger basis set. In any case, the qualitative conclusions reached here from the coarse surfaces in Figures 2 through 6 will not be affected by small changes expected in refined calculations.

Calculations at the MB level used in Figures 2–6 give energies near -1.861 au for geometries close to the 1.27×1.27 Å square, about 5 eV above the ground state. Since the energy of the S state in this approximation is undoubtedly overestimated, continuum excimer emission might be observable at wavelengths longer than 2500 Å. The electronic transition is electric dipole forbidden at a square geometry (G, $^1B_{1g}$; S, $^1B_{2g}$), and rectangular geometries (G, 1A_g ; S, $^1B_{1g}$) but is allowed at geometries of lower symmetry.

In the region of the best geometries for the excimer, the D state lies below the S state, so that radiationless transitions into the D state, and possibly even a radiative transition, need to be considered. The latter is symmetry forbidden at square and rectangular geometries (D, $^1A_{1g}$) but allowed at geometries of lower symmetry. In the MB approximation, the separation of the S and D states at the best excimer geometries is of the order of 1.0–1.5 eV. The exact value is undoubtedly less, which makes an observation of $S \rightarrow D$ emission rather difficult. A reliable determination of the sign and magnitude of the S–D energy difference will require additional calculations with a larger basis set, which are presently under way.

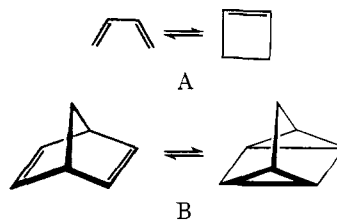
The radiationless process $S \rightarrow D$ may be quite rapid and may quench both excimer emission and the various adiabatic dissociation reactions the excimer might undergo. If the D state

is reached at a geometry near the 1.27×1.27 Å square, several processes appear possible. One is dissociation into four H atoms, i.e., motion along the $R_1 = R_2 = R$ line in Figure 3; another is formation of a diagonal bond yielding a ground state H₂ molecule and two H atoms; still another is formation of both diagonal bonds during an out-of-plane bend leading to formation of two ground state H₂ molecules. Since all of these processes lead downhill on the D surface, there probably will not be time for slower processes such as radiative or radiationless transition to the G state at the original geometry. The latter would otherwise appear quite favorable because of the presence of an avoided crossing.

A transition from either the S or D state to the G state at geometries close to that of the excimer would produce two H₂ molecules in two possible ways and would lead to partial exchange in an $H_2 + D_2^* \rightarrow 2HD$ process. However, such transitions, as well as other processes producing H₂ already noted above, might easily produce molecules which are so hot that they dissociate immediately to H atoms.

In summary, a bewildering variety of photochemical processes seems possible in what would appear to be the simplest bimolecular photochemical process, and that already before much of the six-dimensional hyperspace has been explored or before Rydberg or triplet states have been considered.

Extrapolation to 2s + 2s and Related Pericyclic Processes in Larger Molecules. Processes involving interactions of four electrons in four atomic orbitals are very common in organic photochemistry. If the interaction occurs in a cyclic array of overlapping orbitals, such reactions are called pericyclic.⁵ In general, they involve switching of two bonds, originally connecting atoms A with B and C with D, to connect atoms A with C and B with D. All four orbitals may be of p type, as in cyclobutene \rightleftharpoons butadiene²² (A) and bornadiene \rightleftharpoons quadricyclene²³ (B), but other possibilities exist, e.g., two can be s and



two p, as in propene \rightleftharpoons allene + H₂.²⁴ If the orbitals used are s, or if they are p but the same lobe is used for bonding in the starting material and in the product, the process is referred to as $2s + 2s$.⁵ The case studied here, involving four s orbitals, has more intrinsic symmetry than the others but has the same topology and appears to us to involve the same physical principles. Therefore, we believe that the understanding of the nature of the G, D, and S states which we have achieved for H₄ is illuminating for a discussion of $2s + 2s$ processes in general. Pericyclic reactions may also involve cyclic arrays of other sizes and we shall discuss a generalization later. On the other hand, a four-center reaction need not be pericyclic, e.g., $H_2 + D_2 \rightarrow HD + H + D$.

Today's picture of photochemical $2s + 2s$ processes goes back to Zimmerman,²⁵ who was the first to point out, on basis of MO considerations, that a region of easy return from the excited to the ground state occurs at a "antiaromatic" (in our nomenclature, "biradicaloid") geometry halfway between reactants and products along a $2s + 2s$ and other ground state forbidden reaction paths (in the H₂ + H₂ case, at square geometries). Even earlier, it had been recognized by Abrahamson and Longuet-Higgins²⁶ that orbital correlation, which imposes an energy barrier in the ground state, will not do so in the lowest excited state between the geometry of starting materials and that of products; thus the photochemical process is "orbital symmetry allowed" as a one-step reaction.⁵ This

makes the $2s + 2s$ case similar to $4s + 4s$ and others but different from $2s + 2a$, $2s + 2s + 2s$, and others, as elaborated in detail by Woodward and Hoffmann.⁵ The nature of the electronic states in the antiaromatic, or biradicaloid, region halfway along the concerted reaction path was elucidated by van der Lugt and Oosterhoff²² on the butadiene–cyclobutene case. They used a crude semiempirical calculation for the 4 π electrons involved, starting with VB structures and proceeding to full CI. Their results have been very recently fully confirmed by an ab initio calculation of Grimbert, Segal, and Devaquet.²⁷ Van der Lugt and Oosterhoff pointed out that the minimum in the D state they found at the “halfway” geometry, which we shall refer to in the following as “pericyclic minimum”, is a result of an avoided crossing of two covalent VB structures of the type discussed above, which lead to the G state and the D state, and is therefore likely to occur in $2s + 2s$ and other ground state forbidden pericyclic processes in general. In their opinion, the S state is only accidentally present and therefore the way it correlates between starting materials and products is irrelevant for the photochemical $2s + 2s$ process. It was later pointed out^{14,29,30} that this extreme view is not helpful and that both the minimum in the D state²² and the lack of a barrier in the S state⁵ are important for the existence of the pericyclic photochemical path along the ground state forbidden reaction coordinate, the former providing a minimum and thus a return to the ground state, and the latter providing access to that minimum. In certain cases of $2s + 2s$ reactions large barriers in the S state were actually detected experimentally in agreement with orbital and state correlation diagrams.³¹

The van der Lugt–Oosterhoff mechanism has been criticized as involving a purely hypothetical and unobserved doubly excited state,³² but such states have more recently been observed both in polyenes³³ and in a π -electron biradicaloid molecule.³⁴ Results of another calculation³⁵ failed to produce a minimum in the D state at energies below the S state, perhaps because insufficient extent of CI was used; the D above S ordering was also indicated in the original qualitative diagrams of Abrahamson and Longuet-Higgins.²⁶ The recent ab initio results for butadiene \rightleftharpoons cyclobutene,²⁷ as well as our present results for H_4 , which provide very much the same picture of state surfaces for a rather different chemical system, reaffirm the ordering found by van der Lugt and Oosterhoff²² and indicate that it is probably generally valid for ground state forbidden pericyclic paths such as $2s + 2s$. A more detailed discussion of the present state of understanding of $2s + 2s$ and related pericyclic photochemical processes can be found in ref 36.

In summary, although there is no direct experimental evidence for the detailed mechanism postulated by van der Lugt and Oosterhoff (return to the ground state from a pericyclic minimum in the D state, located at a biradicaloid geometry at which interactions along the bonds to be broken and those to be made are similar in magnitude), it is likely that it is correct. Many of the processes of this type are believed to proceed in a concerted manner (making all of the new bonds while all of the old ones are being broken) because stereochemical information is preserved⁵ (in some cases, a portion of the reaction may proceed in the triplet state, in which loss of stereochemistry is expected on theoretical grounds,¹⁴ so that stereospecificity is not complete). It has been recently pointed out by Kaupp²³ from examination of numerous measured quantum yields that in many reactions of the $2s + 2s$ type an intermediate is most likely present, which partitions between starting materials and products in a way which is independent of whether it was itself prepared from irradiated starting materials or irradiated products. This is just the behavior to be expected for the concerted van der Lugt–Oosterhoff mechanism if the radiationless conversion from the minimum in the D state to the ground state G is not immediate, i.e., if sojourn of the molecule in the minimum in the D state is long enough for loss

of memory and thermal equilibration, but the observation can hardly be taken for a definitive proof of its correctness. Kaupp himself²³ prefers to believe the reaction involves an unsymmetrical (probably ground state) intermediate, whose structure corresponds to our “loose biradicaloid geometry” C A–B D.

There are several questions which one might ask about the detailed mechanism outlined above for the $2s + 2s$ processes, which we believe can be discussed on the basis of our results for H_4 . Obviously, the hypersurfaces calculated in this paper cannot be assumed valid for other $2s + 2s$ processes as they stand. Typically, in addition to the four electrons which are involved in the bond-switching process, there will be others, forming additional bonds, which will prevent many of the total or partial fragmentation processes expected for H_4 . For instance, the uninterrupted downhill slope of the D surface toward four separated atoms will not exist if we consider the face-to-face cycloaddition of two ethylene molecules, since the C–C σ bonds of the two ethylenes will prevent it. As a result, this valley in the D state will be changed into a minimum. Similar considerations will apply in the case of other $2s + 2s$ reactions. With due caution, however, it should be possible to transfer much of the information obtained for H_4 to $2s + 2s$ reactions in general, particularly information having to do with the physical nature of the various excited states and their bonding and antibonding features.

(i) The first question we shall discuss is: why, at the pericyclic biradicaloid geometry halfway through the reaction, is the D state and thus also the pericyclic minimum resulting from the avoided touching of G and D states, below the S state, although simple MO arguments suggest the opposite? If it were not, as was actually suggested originally,²⁶ return at this particular geometry would hardly be expected even though the G state is not far below, since the time spent by the molecule on such a sloping surface would be extremely short, at least in condensed phase, where excess vibrational energy is lost rapidly. Most likely, the molecule would reach some minimum on the S surface, e.g., at starting geometry (possible emission of starting material), or at the product geometry (possible emission of product, actually only very rarely observed³⁷). We believe that the general answer is the same as already given above for the specific case of H_4 ; the simple MO description (3×3 CI) which suggests the order G, S, D is inadequate and needs to be tempered with the simple VB description, providing the order G, D, S in order to understand the order of the three states. The G state is covalent and the S state ionic, as both simple approaches predict, but the D state is of mixed character and neither simple description is correct by itself. It is for this reason that we prefer the G, D, S nomenclature to the otherwise equivalent D (for diradical), Z_1 (for zwitterionic), Z_2 (for zwitterionic) nomenclature used by Salem and collaborators (e.g., ref 28). The partly covalent nature of the D state is particularly clear in the case of butadiene where a correlation can be made with the calculated D state at the planar geometry (unobserved so far), customarily interpreted as two coupled (covalent) triplet ethylenes, based on ab initio and semiempirical calculations.³⁸

It should be noted at this point that other types of biradicaloid minima have been postulated to play a similar role in other classes of photochemical reactions.¹⁴ In many of these, only one low-energy covalent structure can be written for the molecule at the biradicaloid geometry, rather than two, as is the case in pericyclic processes, e.g., for a “broken σ bond” minimum or “twisted π bond minimum”. In such cases, G is covalent, S and D are both ionic, and the G, S, D ordering predicted by simple MO theory^{14,16} is correct (cf. results for stretching of the σ bond in H_2 ^{11,39} and twisting of the π bond in ethylene⁴⁰), and no objection is raised to the D, Z_1 , Z_2 nomenclature.²⁸

(ii) The next question is: what is the role of excimers and

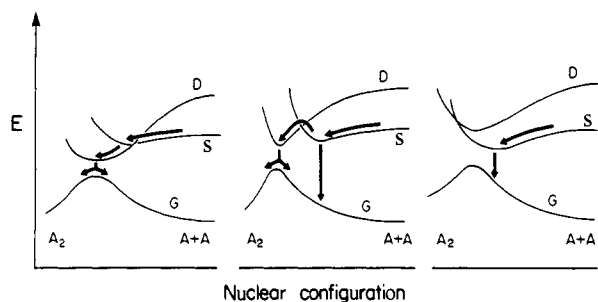


Figure 13. Typical correlation diagrams for ground state forbidden pericyclic reactions of ground (G), singly excited (S), and doubly excited (D) state showing various relative positions of the "excimer minimum" (in S) and the "pericyclic minimum" (in D).

exciplexes in the $2s + 2s$ cycloaddition processes such as olefin dimerization, where are they located on the correlation diagram, and what is their relation to the minimum in the D state through which return to the ground state is believed to occur?

Recent experimental evidence indicates that excimers are intermediates in photochemical cycloaddition reactions in the singlet state,^{41,42} and in at least one case activation energy is needed to proceed from the excimer to products.⁴² Also, simple arguments based on perturbation theory applied to the S state at infinite separation to estimate its relative slope in the direction of products as a function of orientation (regiospecificity, syn-anti specificity) and substitution are quite successful in accounting for the products formed,⁴³ so that it appears that the shape of the S state has some controlling role in these reactions.

We first note that the circumstance that the minimum in the S state of H_4 , corresponding to the H_4 excimer, occurs in the same region of geometries in which the D state undergoes an avoided touching with the G state and has relatively low energy is due to the especially high symmetry of this case: not only does the reaction occur between two identical molecules, but the new σ bonds are entirely equivalent to the old ones because of the lack of directionality of s orbitals, and no other bonds are present. The situation will be different if some or all of the orbitals are of p type. Then, some of the overlaps will be of the more efficient σ type and others of the less efficient π type. Also, the presence of additional bonds in the molecules will make an intimate approach of the two reactants difficult. As a result, the relatively shallow excimer minimum in the S state will be displaced away from the halfway point of the reaction at which the pericyclic minimum in the D state occurs. Indeed, typical excimers²⁰ involve only a slight degree of overlap of the two partners.

Now, displacement away from the halfway point has an unfavorable effect on the energy of the D state, which rapidly rises in energy, and the S state then becomes the lowest excited singlet state. This is less than obvious in the H_4 case, but it must be remembered that in other $2s + 2s$ cases additional bonds will be present which will make the intramolecular distances shorter and the doubly excited D state relatively less favorable (e.g., the σ C-C bond in ethylene). Indeed, experimentally, the excimer state is normally the lowest excited state at the excimer geometry.

Thus, we end up with up to two minima in the lowest excited singlet state of the reacting system along the pericyclic photocycloaddition reaction path (Figure 13). One of these, the excimer minimum, occurs in the S state in a region of relatively large intermolecular separation, where S is lowest, the other, the pericyclic minimum, occurs in the D state halfway through the reaction, where D is lowest. The two minima are distinct in their physical nature, in their function in the photochemical process, and in their position on a correlation diagram (Figure

13). The former is due to exciton and charge-transfer interactions in an ionic excited state, the latter to the presence of an avoided touching in a semiionic semicovalent excited state. Although the physical potential for both minima will exist in any ground state forbidden singlet cycloaddition process such as $2s + 2s$, they may actually not appear in the lowest singlet (S_1) surface, depending on molecular structure. For example, one or both minima may be wiped out by steric repulsions if bulky substituents are present, the excimer minimum might conceivably occur in a higher excited singlet state instead if the lowest excited state is not of "ionic" but "covalent" nature, as happens for some more complicated unsaturated chromophores, or it may also occur so close to the halfway point of the reaction that it would lie above the D state similarly as in H_4 , perhaps because of the presence of some additional bonds in the system which do not permit sufficient separation of the two reacting components (intramolecular photocycloadditions). Similarly, the pericyclic minimum in the D state may lie high above the S state and be of no use in facilitating return to the ground state, etc. Some of these possibilities are shown in Figure 13.

The resulting picture of a typical photocycloaddition reaction with both minima in the lowest excited singlet surface (S_1) then appears as follows. First, a reversible and adiabatic formation of an excimer (exciplex) by populating the minimum in S. If several possible orientations exist, the most stable excimer will predominate, and this is where the simple perturbation theory arguments⁴³ enter. Emission and/or radiationless deactivation to the ground state may occur, leading to re-formation of the starting components since a repulsive section of the G surface is reached in a vertical process.

Second, motion to the pericyclic minimum in the D state halfway along the reaction path, typically over a very small energy barrier formed by a crossing (avoided crossing) of the rising S and decreasing D surfaces as the two components approach closer. The rate of passage over this barrier will co-determine the quantum yield of the photocycloaddition (and regiospecificity) but no simple way of predicting it seems to be available at the moment. It is possible that the sojourn in the pericyclic minimum will be long enough to achieve complete thermal equilibration, and this is suggested by the results of Kaupp.²³ At any rate, radiationless deactivation to the G state will be relatively fast, although return to the excimer or even radiative return to the G state could in principle also occur.

Third, motion on the G surface to the minimum representing product geometry or to the one representing the geometry of the starting materials. Thermal equilibration with the surroundings then completes the primary photochemical process.

One could ask the question whether an analogue of the excimer minimum in the S state could exist for all $2s + 2s$ processes, not only photocycloadditions. Few calculations are available to answer this question and our results for H_4 are, of course, no help. In the butadiene-cyclobutene electrocyclic ring closure no such "intramolecular excimer" minimum has been found.²⁷ We tend to believe at present that these minima do not exist if the interacting components are forced to lie too close to each other, as is the case in cycloreversions, or if their new interaction involves destruction of a previously present interaction, as is the case in the ring closure of butadiene where the π system must be twisted to proceed toward the halfway point for the disrotatory ring closure.

However, it could well be that structural features which would otherwise favor the existence of a well-developed excimer minimum will at least be reflected in the slope of the S surface in the direction toward the half-point of the reaction and facilitate molecular motion along the reaction coordinate. Such an argument is in accordance with the relative success

of simple arguments based on estimated slopes of the **S** surface at the initial geometry.⁴⁴

The proposed mechanism of photocycloadditions provides an immediate physical picture for observations such as the existence of an activation barrier between excimer (exciplex) and product^{41,42} and the lack of simple correlation between exciplex stability and product quantum yield,^{41b} since one barrier and one partitioning lie on the way from exciplex to product (Figure 13). The drastic decrease of both the rate constant k_r for dimer formation from the excimer and that for internal conversion from the excimer to two ground state molecules, k_{ed} , upon going from anthracene to 9,10-dimethylantracene^{41c} can be understood as a consequence of an increase in the barrier between the excimer and the pericyclic minimum, presumably due to steric hindrance, if it is assumed that most of the internal conversion proceeds via the pericyclic minimum, return to the ground state, and dissociation of the partners. If “vertical” internal conversion were negligible, the ratios k_r/k_{ed} (1:5 for anthracene, 1:160 for 9,10-dimethylantracene) would give directly the partitioning ratios for return from the pericyclic minimum to the ground state of reactants and product. Their difference is in the direction expected from consideration of steric hindrance.

(iii) Another question to which our results may be relevant is: in addition to rapid crossing to the ground state surface or returning to the excimer minimum, is there anything else a molecule in a pericyclic minimum in the **D** state would be likely to do? Or, more generally, are there other minima in the **D** state which could be reached, perhaps directly from the initial geometry?

The description of the nature of the **D** state, in particular, the bonding interactions along the diagonals of the H_4 square, indicates that such cross-bonding may be of some generality. It will give rise to a singlet biradical if only one diagonal bond is formed in the cyclic array, in analogy to the decomposition of H_4 square in the **D** state to $H_2 + 2H$, or directly to a ground state product if both diagonal bonds are formed simultaneously. Of course, the ground state singlet biradical with one diagonal bond could close in a second step to produce the same final ground state product, perhaps losing its stereochemistry first, or it could revert back to the starting materials in a fashion familiar from cyclopropylmethyl radical chemistry, conceivably again losing its stereochemistry first. In either case, it is important to note that the **D** state of the starting material correlates with the ground state of the product, so that sooner or later it stops representing the first excited singlet surface S_1 and starts representing the ground state S_0 instead. Obviously, there will be a funnel (touching, or an avoided touching), between the S_1 and S_0 surfaces, and a potentially efficient radiationless deactivation path for a photochemical process. A difficulty with the cross-bonding process would appear to be steric; it seems more difficult to achieve it in organic $2s + 2s$ systems than in the H_4 case, in which no extraneous bonds and atoms need to be considered. The possibility that some of the known singlet state photochemical processes involving cross-bonding can now be ascribed to the propensity of the **D** state for diagonal bonding is presently under scrutiny. E.g., it appears to provide a viable alternative to the recently suggested⁴⁵ “sudden polarization” mechanism for formation of bicyclobutanes and possibly bicyclohexenes from butadienes and hexatrienes in the **S** state (again, we expect that the **D** state is the lower of the two).

(iv) Triplet–triplet annihilation produces excited singlet molecules. What is the place of this process on the correlation diagram, and is it related to the $2s + 2s$ photochemical process?

When two triplet states approach, a coupling into overall singlet, triplet, and quintet is possible. In previous discussions of the overall singlet state,²⁰ statistically formed with 1/9

probability, the fate of the corresponding singlet hypersurface as the two molecules approach to close proximity was not considered. It is now clear that this is the **D** state and that it correlates with the ground state of photochemical products.^{36b} Triplet–triplet annihilation thus appears to be the most direct way to reach the pericyclic minimum in the **D** state and form products, at least in principle. The problem with future experimental investigations of the predicted close relation between triplet–triplet annihilation and photocycloaddition reactions is prevention of competing internal conversion from the high-energy **D** state to one of the lower states and eventually the lowest excited singlet state, before the two interacting molecules even get anywhere near the halfway reaction point. T–T annihilation is believed to occur very fast already at relatively large intermolecular separations,²⁰ indicating that such internal conversion is quite efficient.

Incidentally, the formation of the **D** state from two singly excited triplet molecules clearly demonstrates its doubly excited nature, and this is also true of the other way in which the **D** state might be produced directly, namely two-photon absorption. Obviously, an experimental investigation of processes initiated by direct excitation into the **D** state appears highly promising. The existence of a low-lying state resulting from an overall singlet coupling of two unsaturated bonds approaching each other in their triplet states has been recognized previously.^{46,47}

(v) Why does the photochemical electrocyclic ring opening in the singlet states of 1,4-dewaranthracene and 1,4-dewar-naphthalene give products in their electronically excited states?³⁷

The possibility suggested by the present results is that the state diagram for these very highly exothermic reactions is no different in principle but is distorted since the product side is pulled to lower energies. This distortion will decrease the barrier to thermal ring opening compared with ordinary cyclobutenes and tilt the well present in the **D** state at pericyclic biradicaloid geometry. The well then “spills its contents” and does not hold molecules long enough for efficient radiationless return to S_0 ; instead, some continue on the S_1 surface to product geometry.

(vi) What, if any, is the relation of $2s + 2s$ photochemical processes to doublet–doublet ion recombination reactions, which often produce excited states, and to the equally well-known reverse process?⁴⁸

An approach of two oppositely charged doublet ions $A^+ + B^-$ can give rise to an overall singlet or an overall triplet state (both of these are degenerate if $A = B$). The singlet hypersurface on which random approach will occur with statistical probability 1/4 ordinarily cannot be the ground state surface, which corresponds to an approach of two neutral species, but one of the excited singlet hypersurfaces, S_n . Unless internal conversion to the S_0 surface intervenes, an excited state of the resulting complex will be formed and the ion neutralization reaction is potentially chemiluminescent. Emission may be from an excimer or from either of the two individual components formed by redissociation or by long-range charge neutralization. Obviously, cycloaddition could also result in principle at least by a trivial mechanism from an initially formed ordinary excited state or excimer. Such possible connection between ion neutralization reactions and photochemical processes has been little explored so far.

A natural question to ask is, where does the ion-recombination state belong on the photochemical correlation diagram? The energy of this state is given by the ionization potential and electron affinity of the reactant molecules in the given solvent. In the gas phase, this would be a very highly excited state (typically 7–9 eV for aromatic hydrocarbons). Its energy will be quite sensitive to solvent effects. Clearly, it does not correspond to any of the states already discussed, whose energies

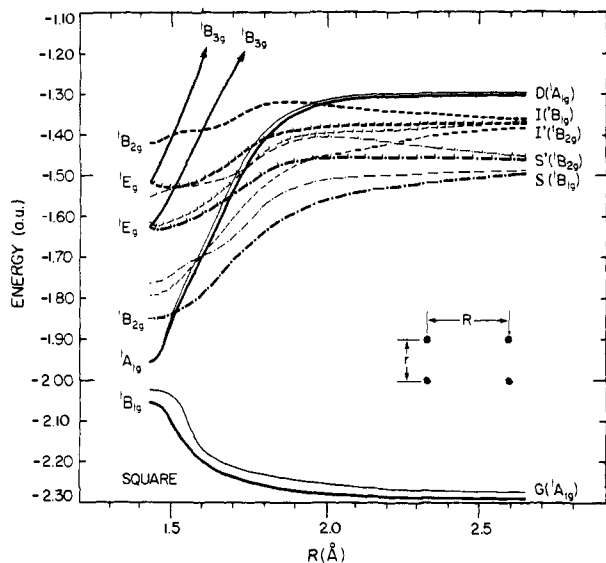


Figure 14. The energy of H_4 in the six lowest states (MB) along the path of best ground state approach of two H_2 molecules from a separation of $R = 2.75 \text{ \AA}$ to the best ground state square ($R = 1.43 \text{ \AA}$). At $R = 2.75 \text{ \AA}$ separation, the H_2 lengths are the equilibrium values ($R_1 = R_2 = r = 0.76 \text{ \AA}$). As the molecules approach, the H_2 lengths increase, reaching $r = 1.43 \text{ \AA}$ at the square. Bold solid lines refer to G and D states (and to two highly excited B_3 states) and thin solid lines to pure G and D configurations without mixing. Bold (thin) dash-dot lines refer to exciton states (configurations), S and S', and bold (thin) dashed lines refer to charge-transfer states (configurations), I and I'. B_2 symmetry is indicated by "tails" added to the dashes in lines belonging to corresponding states or configurations.

approach those of neutral molecular excited states in the limit of infinite separation. Thus, the ion pair state presents a new hypersurface and it is interesting to ask what happens to it as the molecules approach. For H_2 , electron affinity is negative, but it is still possible to identify a state which at least formally corresponds to the pair $H_2^+H_2^- \leftrightarrow H_2^-H_2^+$ at infinite intermolecular separation and to follow it as the molecules approach. While this has no physical meaning for H_4 itself, it can still serve as a model for other ion recombinations of the $2s + 2s$ type.

In order to place the curves corresponding to ion recombination (charge transfer) states on the correlation diagram we have computed and analyzed wave functions at a series of geometries along the best rectangular reaction path for ground state H_2 molecules. Since the equilibrium bond lengths in ionic and excited states of H_2 are longer than that in the ground state, our choice of reaction path causes their energies to appear higher than they would be for a thermally relaxed approach of $H_2 + H_2^*$ or $H_2^+ + H_2^-$. This disadvantage decreases as the reaction coordinate approaches the square geometry, at which even the ground state has relatively long bond lengths. The resulting dips in the energies of all ionic and excited states are clearly seen in the correlation diagram shown in Figure 14. This shows a plot of the energies obtained from MB calculations with 20 configurations. On the right-hand side of the diagram, the already discussed states are identified as G, S, and D. The shape of these three curves is as expected for pericyclic reactions in general from well-known qualitative arguments,^{5,26,36} other approximate calculations,^{22,27} and Figures 2–6. The other exciton state is labeled S'; the ionic states are I and I'. At very large intermolecular separations, S and S' are degenerate, and so are I and I'. The wave functions and their symmetries are approximated as: $\Psi_G^0(1A_{1g}) = X_L \cdot X_R$, $\Psi_S^0(1B_{1g}) = X_L \cdot B_R - X_R \cdot B_L$, $\Psi_S^0(1B_{2g}) = X_L B_R + X_R B_L$, $\Psi_{I'}^0(1B_{1g}) = X_L^+ X_R^- - X_R^+ X_L^-$, $\Psi_{I'}^0(1B_{2g}) = X_L^+ X_R^- + X_R^+ X_L^-$, $\Psi_D^0(1A_{1g}) = b_L \cdot b_R$. Here, X is the covalent valence-bond wave function of the ground state of H_2 ,

X^+ that of the ground state of H_2^+ , X^- that of the ground state of H_2^- , B that of the lowest excited singlet of H_2 , and b that of the lowest excited triplet of H_2 . L and R refer to the left and right H_2 molecules.

At finite intermolecular distances, wave functions for the states of interest can be approximated as linear combinations of the above Ψ^0 's, since mixing with still higher energy terms is relatively unimportant. The functional form of the wave function components X , X^+ , X^- , B , and b is independent of internuclear distances and is dictated by the minimum basis set used, but atomic orbital exponents were reoptimized for each distance (using a separate optimization for the ground state and a separate optimization common to all excited states). The energies of the zero-order wave functions Ψ^0 are shown as thin lines in Figure 14. As expected, exciton splitting increases smoothly with decreasing intermolecular separation. At the same time, the energy of the ionic terms decreases rapidly in approximate accord with the Coulomb potential. In both cases, the antisymmetric ($1B_{1g}$) term is lower in energy.

When interactions between terms of like symmetry are introduced, the thick lines of Figure 14 result. The energy of the ground state is lowered by interaction with highly excited A_1 terms not shown in Figure 14, which introduce some ionic character into the wave function. The interaction between Ψ_S^0 and $\Psi_{I'}^0$ is very strong already at large intermolecular separations and, together with the exciton splitting, is clearly responsible for the deep "excimer" minimum in the S state. This very strong mixing agrees with the usual picture of bonding in excimers already discussed. The higher state resulting from interaction of Ψ_S^0 and $\Psi_{I'}^0$, labeled I in Figure 14, is very strongly destabilized. The terms Ψ_S^0 and $\Psi_{I'}^0$ interact less strongly. The resulting states S' and I', as well as the state I, probably have no minimum near the square geometry when account is taken of the existence of dissociative paths using longer bond lengths.

In answer to the above posed question, our results for H_4 suggest that strong mixing between the zero-order S and I states will be a general feature at least in those cases in which they are not separated in energy by more than a few electron volts and that the ion-pair state I and the exciton state S can only be properly identified as such as fairly large intermolecular separations. We prefer the label excimer (exciplex) state for S, since this term implies the presence of both exciton and charge-transfer interactions. The I surface does not decrease in energy nearly as rapidly as would be expected from a Coulomb potential, and perhaps not at all. The presence of strong mixing (avoided crossing) between zero-order wave functions is also likely to cause facile radiationless transitions from the I to the S surface and vice versa in agreement with observations.

This description obviously contains only some of the basic ingredients of doublet-doublet ion recombination reactions, since the role played by the solvent is not considered.

(vii) What is the relation of the interaction and correlation diagrams constructed using MO's and/or states of the fragments representing partners in cycloaddition reactions⁴³ to the "supermolecule" correlation diagram approach?^{7,5,25,26,36}

In the fragment method, the zero-order wave functions discussed in the preceding section are taken as the basis set for a CI calculation, except that the D state is usually not considered.^{43b} For the $2s + 2s$ case discussed here, the qualitative symmetry arguments and semiquantitative energy estimates used in the fragment methods produce essentially the same interactions among the Ψ_1^0 , $\Psi_{I'}^0$, Ψ_S^0 , and $\Psi_{S'}^0$ terms as obtained by comparison of the thin and thick lines of Figure 14, i.e., a strong stabilization of the lowest of the four states.^{43b} As Figure 14 clearly shows, the interactions are so strong that it would not be wise to use the thin lines as approximations for

the thick ones. Thus, the lowest of the four charge transfer exciton states of the fragment model is identical with the "singly excited singlet state" of the supermolecule model (S). The higher three are believed to be of no importance in photochemical pericyclic processes and are usually not even included in the correlation diagrams constructed by the supermolecule approach. On the other hand, the very important D state of the latter is frequently missing in discussions of the fragment model.^{43b} We feel that this is a very serious omission, leading to incorrect state correlation diagrams.^{43c}

(viii) Finally, it appears likely that the conclusions drawn here can be generalized to other cases of photochemical reactions along ground-state symmetry-forbidden reaction paths such as $4s + 4s$, and we have already done so in some of the preceding discussion. Also, the nature of bonding in the simplest molecular excimer, H_4 , based on both charge transfer and exciton interaction, is probably typical of excimers in general, and even some of the more specific properties, such as easy localizability of excitation in one of the components by a geometrical distortion, and easy distortion from the parallel arrangement of components, may be common. Finally, the course of $2s + 2s$ additions in the ground state, when forced upon the molecule, i.e., formation of one bond followed by a period in which two loose ends of a biradical grope for each other,²¹ is probably shared by other ground-state symmetry-forbidden processes. Our results do not permit us to comment on the present controversy concerning the existence or nonexistence of a shallow local minimum in the ground state in what we calculate to be a very flat region (twixtyl²¹) at open-chain biradicaloid geometries.^{21,49,50}

Acknowledgment. Support of this work by the National Science Foundation (GP-37551) and by grants of computer time received from the Research Committee of the University of Utah and from Washington State University is gratefully acknowledged. One of us (W.G.) expresses his thanks to NATO for a postdoctoral fellowship. J.M. wishes to acknowledge a fruitful role played in formulation of many of the problems addressed in this paper by Professors John I. Brauman (Stanford) and Frank E. Harris (Utah) during an informal "First Random Conference on Organic Chemistry" in a Lake Tahoe summer cabin (October, 1969).

References and Notes

- (1) (a) NATO Postdoctoral Fellow; (b) University of Utah; (c) Washington State University; (d) Alfred P. Sloan Fellow, 1971-1975. Various parts of the results were presented at the American Chemical Society South West Regional Meeting, El Paso, Texas, Dec. 1973, at the International Exciplex Conference, London, Ont., Canada, May 1974 (J. Michl and R. D. Poshusta, "The Exciplex", M. Gordon and W. R. Ware, Ed., Academic Press, New York, N.Y., 1975, p 145), at the Fifteenth Conference on Reaction Mechanisms, Fort Collins, Colo., June 1974, at the Vth IUPAC Symposium on Photochemistry, Enschede, Holland, July 1974 (ref 36b), at the International Symposium on Atomic, Molecular and Solid-State Theory and Quantum Statistics, Sanibel Island, Fla., Jan. 1975, and the VIII International Conference on Photochemistry, Edmonton, Canada, Aug. 1975.
- (2) (a) D. L. Akins, E. H. Fink, and C. B. Moore, *J. Chem. Phys.*, **52**, 1604 (1970); (b) E. H. Fink, D. L. Akins, and C. B. Moore, *ibid.*, **56**, 900 (1972); E. H. Fink, P. Hafner, and K. H. Becker, *Z. Naturforsch.*, **A**, **29**, 194 (1974). Quenching of excited H_2 by ground-state H_2 is also one of the processes postulated to occur during vacuum uv molecular hydrogen laser action: I. N. Knyazev, V. S. Letokhov, and V. G. Movshev, *IEEE J. Quantum Electron.*, **qg-11**, 805 (1975).
- (3) (a) M. Rubinstein and I. Shavitt, *J. Chem. Phys.*, **51**, 2014 (1969); (b) C. F. Bender and H. F. Schaefer, III, *ibid.*, **57**, 217 (1972); (c) C. W. Wilson, Jr., and W. A. Goddard, III, *ibid.*, **56**, 5913 (1972); (d) R. W. Patch, *ibid.*, **59**, 6468 (1973); B. Freihaut and L. M. Raff, *ibid.*, **58**, 1202 (1973); (e) B. M. Gimarc, *ibid.*, **53**, 1623 (1970); (f) H. Conroy and G. Malli, *ibid.*, **50**, 5049 (1969); (g) J. D. Goddard and I. G. Csizmadia, personal communication.
- (4) (a) D. M. Silver and R. M. Stevens, *J. Chem. Phys.*, **59**, 3378 (1973); (b) J. S. Wright, *Can. J. Chem.*, **53**, 549 (1975).
- (5) (a) R. B. Woodward and R. Hoffmann, "The Conservation of Orbital Symmetry", Verlag Chemie, Weinheim, Germany, and Academic Press, New York, N.Y., 1970; (b) for an application to the hydrogen exchange reaction, see R. Hoffmann, *J. Chem. Phys.*, **49**, 3739 (1968).
- (6) H. Eyring, J. Walter, and G. E. Kimball, "Quantum Chemistry", Wiley, New York, N.Y., 1944.
- (7) S. Huzinaga, *J. Chem. Phys.*, **42**, 1293 (1965).
- (8) H. Sambe, *J. Chem. Phys.*, **42**, 1732 (1965).
- (9) R. D. Poshusta and J. Michl, unpublished results.
- (10) W. I. Salmon and R. D. Poshusta, *J. Chem. Phys.*, **59**, 4867 (1973); R. D. Poshusta and D. F. Zetik, *ibid.*, **58**, 118 (1973); R. D. Poshusta and V. P. Agrawal, *ibid.*, **59**, 2477 (1973); R. D. Poshusta and W. F. Siems, *ibid.*, **55**, 1995 (1971); R. D. Poshusta, D. W. Klint, and A. Liberles, *ibid.*, **55**, 252 (1971).
- (11) W. Kołos and L. Wolniewicz, *J. Chem. Phys.*, **41**, 3663 (1964); **45**, 509 (1966).
- (12) G. E. Ewing, *Acc. Chem. Res.*, **8**, 185 (1975); E. Kochanski, B. Roos, P. Siegbahn, and M. H. Wood, *Theor. Chim. Acta*, **32**, 151 (1973).
- (13) L. Salem, "The Molecular Orbital Theory of Conjugated Systems", W. A. Benjamin, New York, N.Y., 1966.
- (14) J. Michl, *Mol. Photochem.*, **4**, 257 (1972).
- (15) J. Kolc and J. Michl, *J. Am. Chem. Soc.*, **95**, 7391 (1973).
- (16) L. Salem and C. Rowland, *Angew. Chem., Int. Ed. Engl.*, **11**, 92 (1972).
- (17) W. J. Hehre, L. Salem, and M. R. Willcott, *J. Am. Chem. Soc.*, **96**, 4328 (1974).
- (18) R. C. Bingham, M. J. S. Dewar, and D. H. Lo, *J. Am. Chem. Soc.*, **97**, 1285 (1975).
- (19) C. R. Flynn and J. Michl, *J. Am. Chem. Soc.*, **96**, 3280 (1974).
- (20) J. B. Birks, "Photophysics of Aromatic Molecules", Wiley-Interscience, New York, N.Y., 1970, p 391.
- (21) R. Hoffmann, S. Swaminathan, B. G. Odell, and R. Gleiter, *J. Am. Chem. Soc.*, **92**, 7091 (1970).
- (22) W. Th. A. M. van der Lugt and L. J. Oosterhoff, *J. Am. Chem. Soc.*, **91**, 6042 (1969).
- (23) G. Kaupp, *Justus Liebig's Ann. Chem.*, 844 (1973).
- (24) W. A. Guillory and S. G. Thomas, Jr., *J. Phys. Chem.*, **79**, 692 (1975).
- (25) H. E. Zimmerman, *J. Am. Chem. Soc.*, **88**, 1566 (1966).
- (26) H. C. Longuet-Higgins and E. W. Abrahamson, *J. Am. Chem. Soc.*, **87**, 2045 (1965).
- (27) D. Grimbert, G. Segal, and A. Devaquet, *J. Am. Chem. Soc.*, **97**, 6629 (1975).
- (28) W. G. Dauben, L. Salem, and N. J. Turro, *Acc. Chem. Res.*, **8**, 41 (1975).
- (29) J. Michl, *Mol. Photochem.*, **4**, 287 (1972).
- (30) J. Michl, *J. Am. Chem. Soc.*, **93**, 523 (1971).
- (31) J. Kolc and J. Michl, *J. Am. Chem. Soc.*, **92**, 4147 (1970); J. Michl, "Chemical Reactivity and Reaction Paths", G. Klopman, Ed., Wiley, New York, N.Y., 1974; J. M. Labrum, J. Kolc, and J. Michl, *J. Am. Chem. Soc.*, **96**, 2636 (1974).
- (32) R. C. Dougherty, *J. Am. Chem. Soc.*, **93**, 7187 (1971).
- (33) B. S. Hudson and B. E. Kohler, *Chem. Phys. Lett.*, **14**, 299 (1972); *Annu. Rev. Phys. Chem.*, **25**, 437 (1974).
- (34) J. Downing, V. Dvořák, J. Kolc, A. Manzara, and J. Michl, *Chem. Phys. Lett.*, **17**, 70 (1972); J. Kolc, J. W. Downing, A. P. Manzara, and J. Michl, *J. Am. Chem. Soc.*, **98**, 930 (1976).
- (35) J. Langlet and J.-P. Malrieu, *J. Am. Chem. Soc.*, **94**, 7254 (1972).
- (36) (a) J. Michl, *Top. Curr. Chem.*, **46**, 1 (1974); (b) J. Michl, *Pure Appl. Chem.*, **41**, 507 (1975).
- (37) N. C. Yang, R. V. Carr, E. Li, J. K. McVey, and S. A. Rice, *J. Am. Chem. Soc.*, **96**, 2297 (1974); R. V. Carr, B. Kim, J. K. McVey, N. C. Yang, W. Gerhartz, and J. Michl, *Chem. Phys. Lett.*, **39**, 57 (1976).
- (38) T. H. Dunning, Jr., R. P. Hosteny, and I. Shavitt, *J. Am. Chem. Soc.*, **95**, 5067 (1973); W. J. Campion and M. Karplus, *Mol. Phys.*, **25**, 921 (1973).
- (39) M. J. S. Dewar and J. Kelemen, *J. Chem. Educ.*, **48**, 494 (1971); A. J. Merer and R. S. Mulliken, *Chem. Rev.*, **69**, 639 (1969).
- (40) U. Kaldor and I. Shavitt, *J. Chem. Phys.*, **48**, 191 (1968).
- (41) (a) Reference 20, pp 319, 629, and 633; J. Sattiel, J. T. D'Agostino, O. L. Chapman, and R. D. Lura, *J. Am. Chem. Soc.*, **93**, 2804 (1971); K. Mizuno, C. Pac, and H. Sakurai, *ibid.*, **96**, 2993 (1974); R. A. Caldwell, G. W. Sovocool, and R. P. Gajewski, *ibid.*, **95**, 2549 (1973); D. Creed and R. A. Caldwell, *ibid.*, **96**, 7369 (1974); R. A. Caldwell and L. Smith, *ibid.*, **96**, 2994 (1974); D. Creed, P. H. Wine, R. A. Caldwell, and L. A. Melton, *ibid.*, **98**, 621 (1976); S. Farid, S. E. Hartman, J. C. Doty, and J. L. R. Williams, *ibid.*, **97**, 3697 (1975); N. C. Yang, D. M. Shold, and J. K. McVey, *ibid.*, **97**, 5004 (1975); N. C. Yang, K. Srinivasachar, B. Kim, and J. Libman, *ibid.*, **97**, 5006 (1975); (b) J. M. McCullough, R. C. Miller, D. Fung, and W.-S. Wu, *ibid.*, **97**, 5942 (1975); (c) A. Castellan, R. Lapouyade, and H. Bouas-Laurent, *Bull. Soc. Chim. Fr.*, 210 (1976).
- (42) J. Ferguson and A. W.-H. Mau, *Mol. Phys.*, **27**, 377 (1974); J. Ferguson and S. E. H. Miller, *Chem. Phys. Lett.*, **36**, 635 (1975). We propose that the "nonfluorescent exact topochemical configuration" of p 638 of this paper is identical with the pericyclic minimum.
- (43) (a) W. C. Herndon, *Top. Curr. Chem.*, **46**, 141 (1974); K. Fukui, *Acc. Chem. Res.*, **4**, 57 (1971); (b) N. D. Epiotis, *J. Am. Chem. Soc.*, **94**, 1946 (1972); *Angew. Chem., Int. Ed. Engl.*, **13**, 751 (1974); (c) N. D. Epiotis, R. L. Yates, D. Carlberg, and F. Bernardi, *J. Am. Chem. Soc.*, **98**, 453 (1976).
- (44) A. Devaquet, *J. Am. Chem. Soc.*, **94**, 5626 (1972).
- (45) W. G. Dauben and J. S. Ritschner, *J. Am. Chem. Soc.*, **92**, 2925 (1970); V. Bonacić-Koutecký, P. Bruckmann, P. Hiberty, J. Koutecký, C. Leforestier, and L. Salem, *Angew. Chem.*, **87**, 599 (1975); P. Bruckmann and L. Salem, *J. Am. Chem. Soc.*, in press.
- (46) J. Koutecký and J. Paldus, *Theor. Chim. Acta*, **1**, 268 (1963).
- (47) E. M. Evleth and G. Feler, *Chem. Phys. Lett.*, **22**, 499 (1973).
- (48) For leading references, see G. J. Hoytink, "Chemiluminescence and Bioluminescence", M. J. Cormier, D. M. Hercules, and J. Lee, Ed., Plenum Press, New York, N.Y., 1973, p 147; A. Weller and K. Zachariasse, *ibid.*, p 181; A. J. Bard, C. P. Kresztelyi, H. Tachikawa, and N. E. Tokel, *ibid.*, p 193; A. Weller, "5th Nobel Symposium", S. Claesson, Ed., Interscience, New York, N.Y., 1967, p 413; M. Ottolenghi, *Acc. Chem. Res.*, **6**, 153 (1973); K.-D. Gundermann, *Top. Curr. Chem.*, **46**, 61 (1974); T. J. Chuang and K. B. Eisenthal, *J. Chem. Phys.*, **62**, 2213 (1975); N. Mataga, "The Exciplex", M. Gordon and W. R. Ware, Ed., Academic Press, New York, N.Y., 1975, p 113.
- (49) G. A. Segal, *J. Am. Chem. Soc.*, **96**, 7892 (1974).
- (50) M. J. S. Dewar and S. Kirschner, *J. Am. Chem. Soc.*, **96**, 5246 (1974).